1

2

Oral tribology: providing insight into oral processing of food colloids

5

Anwesha Sarkar[1][*][†], Siavash Soltanamadi[1][†], Jianshe Chen[2] and Jason R Stokes[3]

[1]Food Colloids and Bioprocessing Group, School of Food Science and Nutrition, University of Leeds, UK

[2]School of Food Science and Biotechnology, Zhejiang Gongshang University, Hangzhou, 310018, China

[3]School of Chemical Engineering, The University of Queensland, Brisbane, QLD, 4072, Australia

*Corresponding author:

Prof. Anwesha Sarkar

Food Colloids and Processing Group,

School of Food Science and Nutrition, University of Leeds, Leeds LS2 9JT, UK.

E-mail address: A.Sarkar@leeds.ac.uk (A. Sarkar).

†The authors contributed equally: Anwesha Sarkar and Siavash Soltanahmadi

27

28 **Highlights**

29 • Evolution of use of oral tribology in food colloid science is presented

30 • Key lubrication theories relevant to complex food fluids are covered

31 • Current applications of tribology specific to food colloid research are discussed

32 • Advanced complementary techniques to uncover frictional dissipation are examined

33 • Tribology may help addressing food safety/ sustainability challenges in the future

34

Graphical Abstract
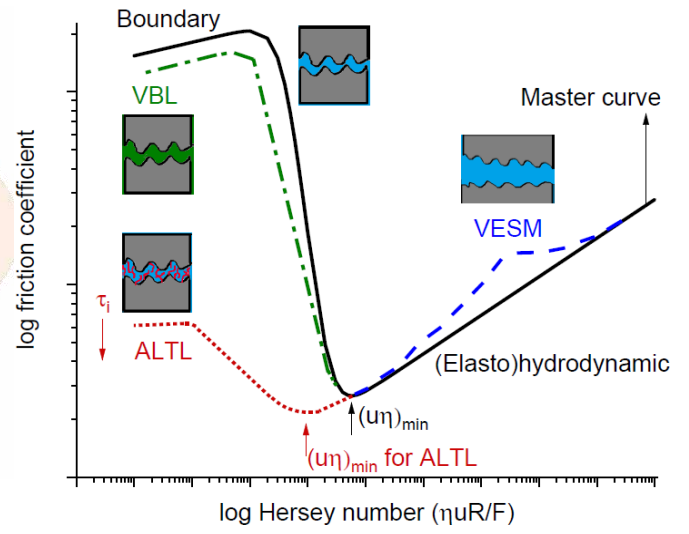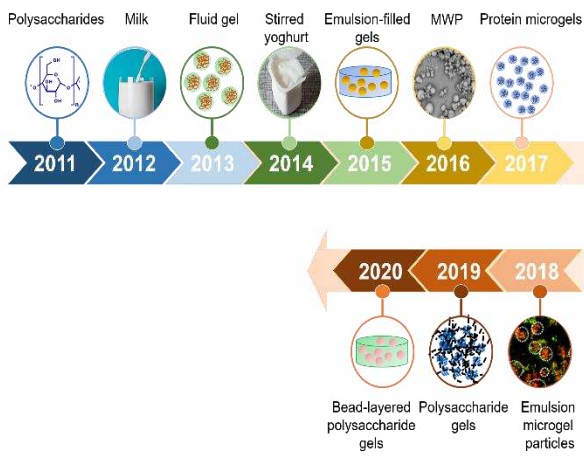
Abstract

Food oral processing research has attracted a great deal of attention in the last few decades owing to its paramount importance in governing sensory appreciation and pleasurable experience of consuming foods and beverages and eventually regulating nutrient intake. A range of physiologically-controlled unit operations from first bite, to particle size reduction, mastication with saliva, bolus formation, swallowing to generation of oral residues occur during oral processing of solid foods across a range of time and length scales resulting in various physical, biochemical and psychological consequences. Tribology is the study of friction and lubrication, and it has emerged as a key tool to deconvolute these complex processes and provide insights into the physics of oral processing and sensory perception. This review provides an overview of "oral" tribology including experiments in the last decade on food colloids and lubrication theories, and highlights a perspective on how the field is evolving to address various food science challenges. This includes current and forecast future applications of tribology in designing healthier foods, creating sustainable alternatives without compromising mouthfeel, tackling food counterfeiting and tailoring foods for aging populations. We also examine a suite of advanced complementary techniques such as imaging, scattering, and adsorption using specific examples from allied fields that would be useful to uncover frictional dissipation in food systems in the future. The perspectives provided in this review thus represent an exciting glimpse of what tribology can offer, which may become a routine and integral step in food colloidal design in the future.

Keywords: Oral tribology; Stribeck curve; lubrication; biopolymer; rheology; adsorption

1. Introduction

Historically, food colloid science has been dedicated to developing structure-property relationships controlling the stability of colloidal ingredients and complex multiphasic food structures during processing and storage. Due to the continuous rise in food-linked diseases, such as obesity and cardiovascular diseases, there has been an upsurge in research interests in the colloids community over the last few decades to investigate interaction of food colloids with various physiological sites within the human body. There is now a consensus that food undergoes a series of complex transformation across a range of time and length scales in the mouth upon consumption. In addition, the heat and mass transport phenomena occurring in mouth influence the dynamic hedonic appreciation (Chen, 2009; Selway & Stokes, 2014). The multi-scale transformation of food and the oral transit time not only affect the psychological aspects of sensory perception but also impact the physiological biomarkers governing nutrient intake and oro-sensory satiety (Campbell, Wagoner, & Foegeding, 2017; Hetherington, 1996; Krop, Hetherington, Miquel-Kergoat, & Sarkar, 2018; Stribiţcaia, Evans, Gibbons, Blundell, & Sarkar, 2020a). Particularly, the change in length-scale *i.e.* the film thickness of food/ food-salivary film between the oral surfaces is proposed as a key factor. It is postulated that oral processing involves gradual transition of regimes where the bulk fluid properties govern the sensory outputs such as thickness, to one where surface interaction-induced tribological properties tend to dominate the mouthfeel perception, such as smoothness (Chen & Stokes, 2012; Kokini & Cussler, 1983; Pascua, Koç, & Foegeding, 2013).

Food oral processing of solid foods includes six essential unit operations ranging from first bite, comminution, granulation involving food particle-saliva as well as food particle–surface interactions, bolus formation, swallowing to post swallowing generation of oral residues, and the transformation of food during this sequence is suggested to relate to the temporal sensory perceptions of texture, taste and aroma (Stokes, Boehm, & Baier, 2013).

Although oral processing research has existed for several decades (Hutchings & Lillford, 1988; Prinz & Lucas, 1997), the timely review by Chen (2009) summarizing the oral physiology and rheological aspects of food in the oral regime as well as swallowing helped stimulate a renaissance in research interests in food oral processing among the colloid scientists.

If we dissect the food oral processing research domain, it includes four main subareas, 1) oral behaviour including chewing (Brown, Eves, Ellison, & Braxton, 1998; Foster, et al., 2011; Prinz & Lucas, 1997; Wilson, Luck, Woods, Foegeding, & Morgenstern, 2016) 2) food bolus rheology (Devezeaux de Lavergne, van de Velde, & Stieger, 2017; Foegeding, et al., 2011; Nishinari, Fang, & Rosenthal, 2019; Stokes, et al., 2013; Witt & Stokes, 2015), 3) food-saliva interaction (Mosca & Chen, 2017; Sarkar, Ye, & Singh, 2017b), and 4) sensory perception (Chen, 2014; Palczak, Blumenthal, Rogeaux, & Delarue, 2019; Pascua, Koç, & Foegeding, 2013; Schlich, 2017), of course, not in any particular order. In addition, the allied areas impact of food oral processing on food intake/ satiation/ satiety and, as well as role of oral processing in nutrient digestion (*in vitro* and *in vivo* studies) and their metabolic responses. However, a paradigm shift in the field of oral processing to include the fifth indispensable aspect *i.e.* oral tribology involving the study of oral friction, lubrication and wear can be noticed now with exponential growth of research output numbers and citations.

The pioneering work nearly 44 years ago (Kokini, Kadane, & Cussler, 1977) highlighted the importance of oral tribology to govern some of the key organoleptic properties such as smoothness, slipperiness, which could not be described by instrumental rheological characterization alone. In the early 21st century, this work has been sporadically followed by tribology of saliva (Bongaerts, Fourtouni, & Stokes, 2007), chocolates (Lee, Heuberger, Rousset, & Spencer, 2004), tea (Rossetti, Bongaerts, Wantling, Stokes, & Williamson, 2009), model hydrocolloids particularly in the fluid film regimes (de Vicente,

Stokes, & Spikes, 2006), nonionic polyoxyethylene surfactants (Graca, Bongaerts, Stokes, & Granick, 2007) and emulsions (Malone, Appelqvist, & Norton, 2003). Nevertheless, the last ten years captured in **Figure 1** shows a systematic progress in oral tribology of food colloids and colloidal ingredients from various research groups across the globe focusing on food polysaccharides, proteins, gels, microgels and fluid gels, emulsion microgels to foods such as yoghurts, cheese *etc.* Of course besides these major developments highlighted in **Figure 1**, elegant progress has been made in tribological understanding of complex emulsions (Douaire, Stephenson, & Norton, 2014; Oppermann, Verkaaik, Stieger, & Scholten, 2017), iso-rheological semi-solid colloids (Laguna, Farrell, Bryant, Morina, & Sarkar, 2017a; Selway & Stokes, 2013) and solid foods (Kim, et al., 2020). Therefore, this appears as an opportune time to write a review on oral tribology of food colloids in this 35th Anniversary Issue of *Food Hydrocolloids*.
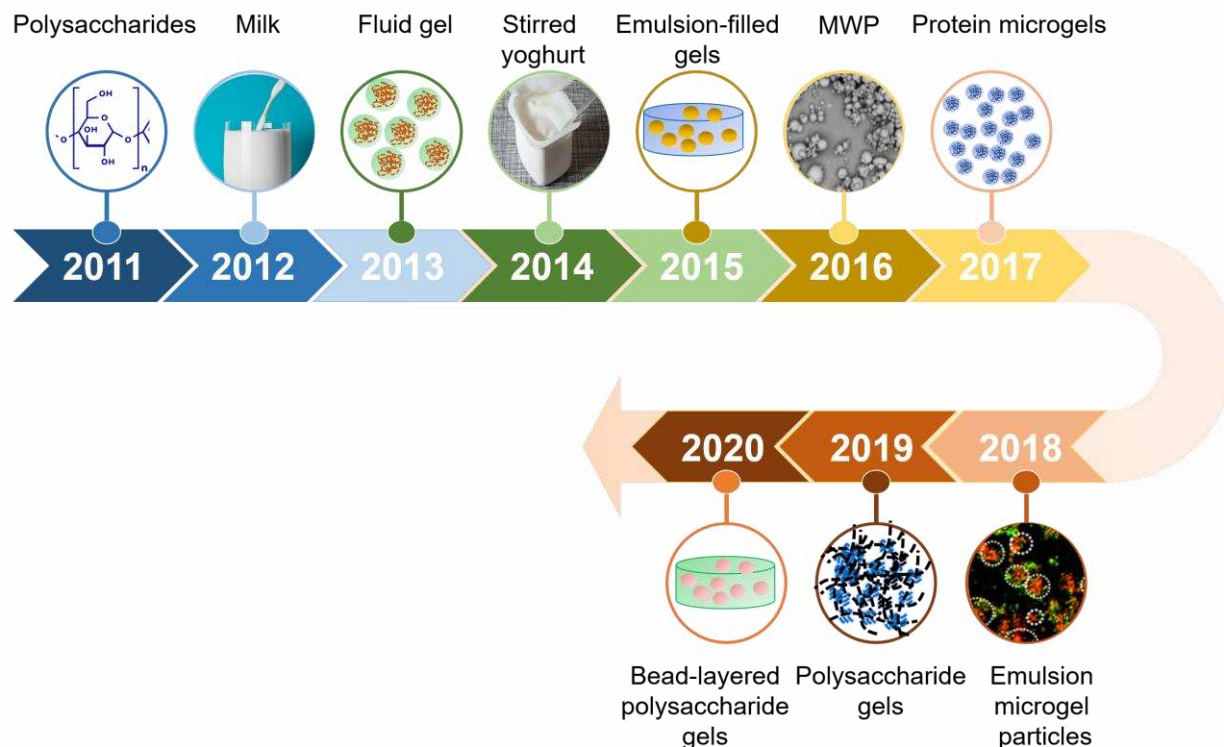
Figure 1. Major developments in tribology of colloidal ingredients, model systems and real food in the last ten years. The development in each year is considered to be major depending upon the new insights generated in tribology of colloid (with > 20 citations in Google Scholar) except the 2020 article. Any development on new tribological device or surface is not included. The timeline shows tribological characterization of

polysaccharides, such as pectin, xanthan gum, gellan, and locus bean gum (Stokes, Macakova, Chojnicka-Paszun, de Kruif, & de Jongh, 2011), milk with a fat content ranging between 0.06 and 8 wt% (Chojnicka-Paszun, de Jongh, & de Kruif, 2012), κ-carrageenan-based fluid gel (Garrec & Norton, 2013), stirred yoghurt testing effects of fat, protein, and casein to whey protein ratio (Sonne, Busch-Stockfisch, Weiss, & Hinrichs, 2014), fat droplets dispersed in emulsion-filled gels (Liu, Stieger, van der Linden, & van de Velde, 2015), microparticulated whey protein (MWP) dispersed in liquids or gels (Liu, Tian, Stieger, van der Linden, & van de Velde, 2016), whey protein microgels testing effects of volume fraction and surfaces (hydrophilic/hydrophobic) (Sarkar, Kanti, Gulotta, Murray, & Zhang, 2017a), emulsion microgel particles (Torres, Andablo-Reyes, Murray, & Sarkar, 2018), polysaccharide gel boli with model saliva (Krop, Hetherington, Holmes, Miquel, & Sarkar, 2019) and bead-layered hydrogel boli with model saliva (Stribiţcaia, Krop, Lewin, Holmes, & Sarkar, 2020b).

The present review thus focuses on the oral tribology of food colloids with a clear emphasis of providing perspectives on future research. Oral tribology has a huge potential for designing biophysically informed food colloids in the future in a cost-effective manner, but effective mimicking of the complex features, deformability and motions of oral surfaces to perform tribological experiments and harmonization of such surfaces to answer specific questions are still needed to enable its widespread use. Although there has been growing interests in designing new tribometers with continual attempts to emulate oral tongue surface in terms of softness, wettability and roughness (Andablo-Reyes, et al., 2020; Bongaerts, et al., 2007; Carpenter, et al., 2019; Rudge, Scholten, & Dijksman, 2020; Sarkar, et al., 2017a; Taylor & Mills, 2020) using a variety of tribological or custom-made rheological set-ups or altering motions in the set ups (Andablo-Reyes, et al., 2020; Fuhrmann, Aguayo-Mendoza, Jansen, Stieger, & Scholten, 2020; Mo, Chen, & Wang, 2019; Tsui, Tandy, Myant, Masen, & Cann, 2016; Wang, Wang, & Chen, 2021), such designs and improvements in tribological set ups are considered to be beyond the scope of this article. We also do not cover salivary tribology or food-saliva interactions in this article as this topic has been extensively covered in recent reviews (Boehm, Yakubov, Stokes, & Baier, 2020; Mosca & Chen, 2017; Sarkar, Andablo-Reyes, Bryant, Dowson, & Neville, 2019a; Sarkar & Singh, 2012; Sarkar, Xu, & Lee, 2019b; Sarkar, et al., 2017b). The comprehensive reviews on rheological to tribological transition during oral processing and analysis of various lubrication regimes as well as growing importance of tribology to study food oral processing (Chen & Stokes, 2012; Sarkar, et al., 2019a; Selway & Stokes, 2014; Shewan, Pradal, & Stokes,

2019) as well as reviews on tribology-sensory relationship (Pradal & Stokes, 2016; Prakash, Tan, & Chen, 2013; Sarkar & Krop, 2019; Stokes, et al., 2013) facilitate this current article.

Here, we aim to provide a different perspective to previous reviews by focusing on the theories of lubrication and soft tribology, and highlighting some important models that are seldom used to discuss experimental tribological results in the food community. We anticipate that this section on lubrication theories should enable making quantitative elucidation of tribological regimes and lubrication mechanisms of complex food fluids, which often get underestimated in food colloid science literature. We also direct our attention to how tribology can be used to address various food-linked challenges ranging from designing healthier colloids, addressing food sustainability, detect food counterfeiting as well as designing food for vulnerable population using specific case studies from literature. Finally, we examine several ancillary techniques drawing inspiration from other fields that could benefit unravelling various lubrication mechanisms occurring in complex multiphasic food colloidal systems. We hope the article written in an opinion style particularly outlining the future of tribology in food applications will entice colloid scientists to use tribology as a mechanical tool answering mechanistic questions behind the sensory appreciation of food.

Table 1. List of abbreviations and symbols.

Acronyms	Full form	Symbols	Definition
AFM	Atomic force microscopy	h_{min}	Minimum lubricant film thickness
ALTL	Adsorbed lubricious thin layers	E'	Equivalent modulus of elasticity
BE	Binding energy	E_0	Rubbery elastic modulus
BGG	Bovine gamma-globulin	E_∞	Glassy elastic modulus
BSA	Bovine serum albumin	H_c	Central dimensionless film thickness
BSM	Bovine submaxillary mucin	H_{min}	Minimum dimensionless film thickness
CD	Circular dichroism	R'	Effective radius of curvature
DLS	Dynamic light scattering	R_a	Centre line average roughness
EHL	Elasto-hydrodynamic lubrication	R_q	Mean square roughness
HA	Hydroxyapatite	d_{50}	Median diameter
HD	Hydrodynamic	u_c	Critical entrainment speed
IDDSI	International dysphagia diet standardisation initiative	η_{eff}	Effective viscosity
LF	Lactoferrin	μ_0	Friction coefficient in the speed-independent regime
MTM	Mini traction machine	μ_{EHL}	Friction coefficient in EHL regime
MWP	Microparticulated whey protein	σ_c	Composite surface roughness

PDMS	Polydimethylsiloxane	τ_i	Interfacial shear strength
ppm	Parts per million	ΔD	Dissipation shift
QCM-D	Quartz crystal microbalance with dissipation monitoring	Δf	Frequency shift
SAXS	Small angle X-ray scattering	h	Lubricant film thickness
SE	Spectroscopic ellipsometry	η	Viscosity
SPR	Surface plasmon resonance	E	Modulus of elasticity
SRR	Slide-to-roll ratio	F	Normal load
SUP	Supercharged polypeptides	H	Dimensionless film thickness
UHMWP	Ultra-high-molecular-weight polyethylene	R	Radius of curvature
UN	United nation	T	Time
VBL	Viscous boundary layer	U	Dimensionless speed parameter
VESM	Viscoelasticity of soft material	W	Dimensionless load parameter
XPS	X-ray photoelectron microscopy	k	Ellipticity parameter
		p	Pressure
		t	Viscoelastic relaxation time scale
		u	Entrainment speed
		δ	Indentation/deformation depth
		λ	Dimensionless film thickness parameter
		μ	Friction coefficient
		ξ	Mesh size of a hydrogel network
		σ	Surface roughness
		τ	Shear stress
		υ	Poisson ratio

181

2. Theories of lubrication

183 Classical theories of lubrication define four regimes of lubrication which are boundary,

184 mixed, elasto-hydrodynamic (EHL) and hydrodynamic (HD). The transition between regimes

185 has often been defined qualitatively through changes in the friction coefficient values in the

186 form of a Stribeck curve (**Figure 2**), which presents data as a function of speed-dependent

187 parameter that is related to the film thickness between substrates (Bongaerts, et al., 2007;

188 Hamrock, 1994; Stribeck, 1902). In common practice, the minimum film thickness (h_{min}), in

189 a lubricated contact, is calculated assuming smooth surfaces and hence ignoring the

190 influence of surface texture. The surface texture principally is important when contact

191 surfaces are in close proximity, where opposing asperities (*i.e.* peaks of the surface

192 roughness) encounter direct contacts. Therefore, tribologists defined a dimensionless film

193 thickness parameter (λ) which encompasses the influence of surface roughness (σ) and

194 provides an indication of the overall degree of direct asperity contact. To incorporate the

195 impact of surface roughness of both contact bodies (σ_1 and σ_2), a parameter has been

10

196   derived and referred to as combined or composite surface roughness (σ_c). λ is given by

197   equation (1) (Hamrock, 1994).

198

$$\lambda = \frac{h_{min}}{\sigma_c} \text{ and } \sigma_c = \sqrt{\sigma_1^2 + \sigma_2^2} \tag{1}$$

199

200   In common practice, σ in equation (1) has been represented by roughness parameters

201   including the mean square roughness (R_q) or the centre line average roughness (R_a). Tall

202   asperities has more pronounced impact on R_q value than on R_a value. Therefore, R_q is more

203   often used in tribology and theoretical studies as opposed to R_a, latter *is* commonly relevant

204   for manufacturing of engineering parts such as quality assessment reports. A tribo-contact

205   operating at $\lambda < 1$ (a high degree of contact expected to occur between the surfaces) and

206    $\lambda > 10$ (the minimum possibility of surface contact) is generally attributed to boundary

207   regime and hydrodynamic lubrication regimes respectively (Hamrock & Dowson, 1981).

208   Upon increase of λ to values over 1, one expects to gain contribution of the fluid film to load

209   bearing and, thereby reduction in the direct contact between surfaces. The elasto-

210   hydrodynamic (EHL) lubrication regime exploits elastic contribution of contact bodies and

211   occurs just before the HD regime where full-film lubrication is developed. As shown in **Figure**

212   **2** using a black solid line, the friction coefficient increases in the hydrodynamic regime as

213   the lubricant film grows thicker.

214
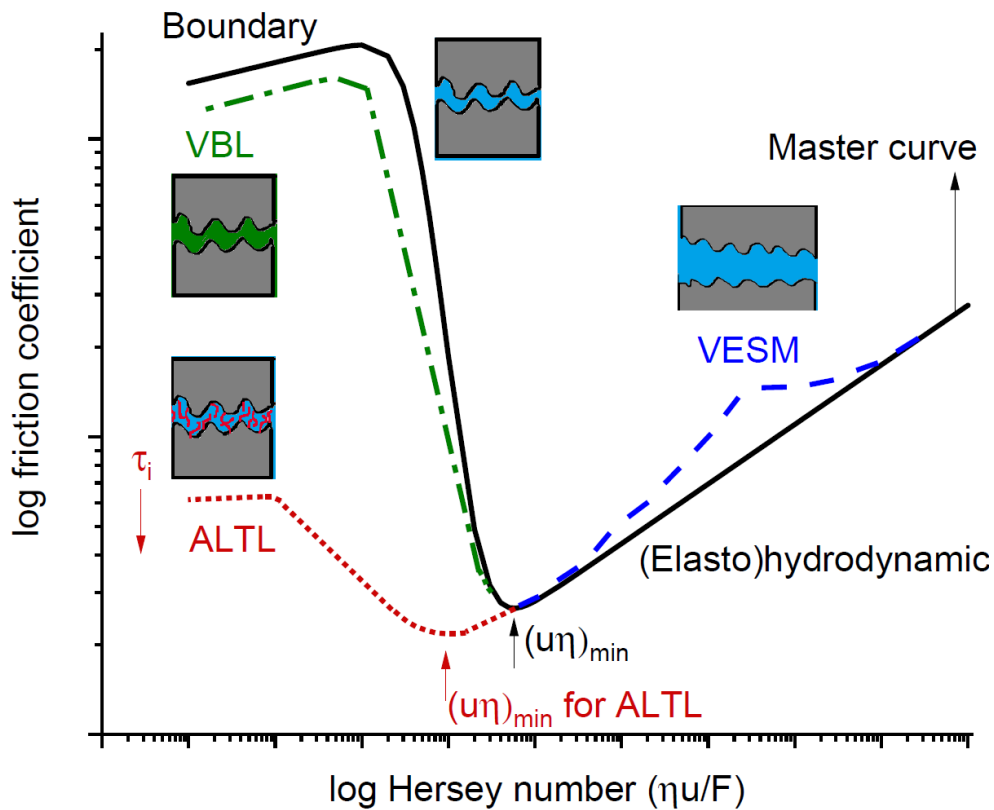
Figure 2. A typical Stribeck curve is presented in black line. The influence of viscoelasticity of soft material (VESM) on the friction coefficient of the EHL regime is shown in dashed blue line. The lubricant retention at the contact interface through a viscous boundary layer (VBL) of a viscous lubricant is shown in dash-dotted green line. Adsorbed lubricious thin layers (ALTL) has considerable influence on the lubrication performance in the mixed and boundary regime and this influence is demonstrated using a dotted red line. Friction coefficient is obtained by dividing the frictional (lateral) forces by the normal load. The Hersey number ($\eta u/F$) is a dimensionless parameter initially designed for journal bearing application. The Hersey number is the product of the lubricant viscosity (η), entrainment speed (u) and the contact load per unit of contact radius (F). Therefore, the Hersey number embraces the influence of fluid viscosity and the contact load (provided the film thickness remains constant by change of load) and displays the influence of speed change on frictional forces.

In lubrication theory when the contacting surfaces are fully separated by a lubricant film (*i.e.* full-film lubrication), further classifications are conducted to illuminate the influence of material elasticity and viscous behaviour of the lubricant on the lubricant film thickness. These are addressed in the following section.

Isoviscous elastic lubrication regime. In the full-film lubrication, the influence of material elasticity and fluid viscosity effects demarcate four types of full-film lubrication regimes especially observed in elliptical contacts. These are isoviscous-rigid, viscous-rigid, elastohydrodynamic of materials with low elastic-modulus (*i.e.* isoviscous-elastic) and

237   viscous-elastic (Hamrock & Dowson, 1978b). These regimes are distinguished based on the

238   influence of contact pressure on the magnitude of solid elasticity and lubricant viscosity

239   (Hamrock & Dowson, 1978b) with the isoviscous-elastic regime probably being the most

240   prevalent condition in the oral tribology considering the relatively low contact pressures (30-

241   50 kPa) and shear and elastic moduli in the oral processes (tongue's shear modulus of 2.5

242   kPa) (Sarkar, et al., 2019a). The compression tests on pig's tongue samples have suggested

243   an elastic modulus of around 2.5-15 kPa (Andablo-Reyes, et al., 2020; Dresselhuis, de

244   Hoog, Cohen Stuart, & van Aken, 2008).

245   The governing equations to calculate the isoviscous-elastic fluid-film thickness ($H =$

246    $\frac{h}{R'}$) for soft elliptical contacts are given by equations (2) and (3) (Hamrock & Dowson, 1978a):

247

$$H_{min} = 7.43(1 - 0.85e^{-0.31k})U^{0.65}W^{-0.21} \qquad (2)$$

$$H_c = 7.32(1 - 0.72e^{-0.28k})U^{0.64}W^{-0.22} \qquad (3)$$

248

249   where, H is dimensionless film thickness, h is the film thickness, U is dimensionless speed

250   parameter ($\frac{u\eta}{E'R'}$), W is dimensionless load parameter ($\frac{F}{E'R'^2}$) and k is the ellipticity parameter,

251   latter is the ratio of the semi-major axis to the semi-minor axis of the contact ellipse. Terms

252   u, η and F are the mean surface velocity (entrainment speed), viscosity of the fluid and the

253   normal applied load. R' and E' are the effective radius of curvature in the direction of the

254   fluid entrainment and the equivalent modulus of elasticity of contacting bodies respectively.

255   R' and E' are given by equation (4):

256

$$\frac{1}{E'} = \frac{1}{2}\left(\frac{1 - v_1^2}{E_1} + \frac{1 - v_2^2}{E_2}\right) \ and \ \frac{1}{R'} = \frac{1}{R_1} + \frac{1}{R_2} \qquad (4)$$

257

258　　where, (E_1, E_2), (v_1, v_2) and (R_1, R_2) are the elastic moduli, Poisson's ratios and the radii of

259　　curvature respectively of the two contact bodies (1 and 2). A k value of 1 defines circular

260　　contacts and values above 2 represent contact configurations approaching line contacts of

261　　soft elastic bodies (see **Figure 3**). This indicates that the film thickness grows towards that

262　　of the line contact with an increase in the ellipticity parameter, provided that dimensionless

263　　speed, load, and material parameters (the equivalent modulus of the bodies and the

264　　pressure-viscosity coefficient of the lubricant) remained constant. k is a function of the

265　　principal radii of the contacting bodies and can be predicted using the following empirical

266　　equation (equation (5)) (Brewe & Hamrock, 1977):

267

$$k = 1.0339(\frac{R'_x}{R'_y})^{0.636} \tag{5}$$

268　　where, R'_x and R'_y denote the effective radius of curvature in x and y direction of the

269　　coordinate systems, respectively.
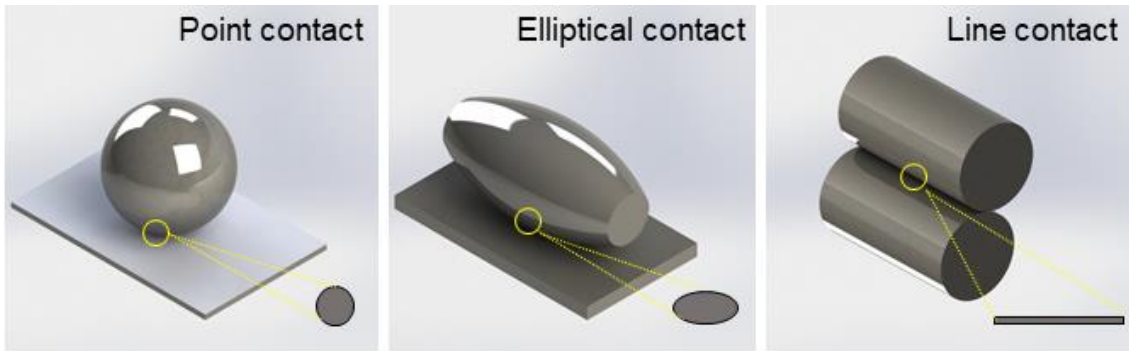
271
272　**Figure 3.** Illustration of contact configurations and resultant point (k=1), elliptical (k≠1 and<12) and line (k>12)
　　contacts.
273

274　　　　The film thickness equations can be derived by solving Reynolds equation taking into

275　　account the material compressibility and the fluid viscous effects when the entrainment

276　　occurs along the minor axis of the contact ellipse allowing the minimum film thickness to

277　　take place at the contact centre-line (Hooke, 1995). The extent of contact deformation and

14

278 entrainment direction can shift the place where the minimum film thickness takes place and

279 hence altering the governing equations (de Vicente, Stokes, & Spikes, 2005; Hooke, 1995).

280   de Vicente, et al. (2005) numerically solved a 2D problem of Reynolds equation and

281 the elasticity equation simultaneously for a fully-flooded point contact lubricated with

282 Newtonian fluids. In solving Reynolds equation, it was assumed that the contact bodies have

283 velocity vectors only in the direction of the lubricant entrainment and the action of the

284 squeeze film ($12\eta \frac{\partial h}{\partial T}$, T is $time$) is negligible. The obtained film thickness equations for

285 isoviscous-elastic point contact ($k = 1$) are shown in equations (6) and (7):

286

$$H_{min} = 2.8U^{0.66}W^{-0.22} \qquad (6)$$

$$H_c = 3.3U^{0.60}W^{-0.14} \qquad (7)$$

287

288   The relations showed relatively good agreement with equations (2) and (3) (Hamrock

289 & Dowson, 1978a), except a weaker load dependence in the case of central film thickness.

290 An experimental work, however, showed that the theoretical models may overestimate the

291 film thickness and following equations (equations (8) and (9)) were showed the best fit for

292 results obtained in the study (Myant, Fowell, Spikes, & Stokes, 2010):

293

$$H_{min} = 2.8U^{0.68}W^{-0.20} \qquad (8)$$

$$H_c = 3.3U^{0.63}W^{-0.13} \qquad (9)$$

294

295   Integration of viscous shear stress over the contact area of the interface yields the

296 viscous friction force acting on each surface which then can be converted into the friction

297 coefficient by dividing that by the normal force. Assuming the lubricant film is thin (no

298 gradient of pressure, p, in the direction perpendicular to the lubricant entrainment), viscous

299   shear forces (τ) for Newtonian fluids on each contact body (*1* is the upper body and *2* is the

300   lower body) can be calculated using equation (10):

301

$$\tau_1 = -\left(\frac{u_1 - u_2}{h}\right)\eta - \frac{h}{2}\frac{\partial p}{\partial x} \ and \ \tau_2 = \left(\frac{u_1 - u_2}{h}\right)\eta - \frac{h}{2}\frac{\partial p}{\partial x} \tag{10}$$

302

303   In the work by de Vicente, et al. (2005), prediction of friction, therefore, was carried

304   out through integration of velocity-dependent (Couette flow, $\tau_{Couette} = \frac{\Delta u}{h}\eta$) and pressure-

305   dependent (Poiseuille flow, $\tau_{Poiseuille} = \frac{h}{2}\frac{\partial p}{\partial x}$) shear stresses. The regression fitting of the

306   data brought about equation (11), provided that the contact is immersed in a lubricant bath

307   filling the diverging region of the contact:

308

$$\mu = 1.46U^{0.65}W^{-0.70} + SRR(3.8U^{0.71}W^{-0.76} + 0.96U^{0.36}W^{-0.11}) \tag{11}$$

309

310   where, SRR denotes slide-to-roll ratio between two bodies (1 and 2) which is presented in

311   equation (12):

$$SRR = \frac{|u_1 - u_2|}{u_{entrainment}} \tag{12}$$

312

313   Care has to be taken in using this equation as to the Hertzian deformation being small

314   enough relative to the material thickness which satisfies the assumption of bulk elastic

315   material (de Vicente, et al., 2005). Masticatory and biting forces on the teeth are shown to

316   be in the range of 0.05-0.1 kN and 0.2–2 kN (Sessle, 2014). Also, able-bodied individuals

317   were observed to be capable of applying forces in the range of 13 N (Robinovitch, Hershler,

318   & Romilly, 1991). Assuming similar masticatory forces on tongue (50 N) and load-applying

319   capability of tongue (13 N), popcorn kernels with a diameter of around 5 mm and an elastic

320 modulus of 325 MPa (Williams, Wright, Truong, Daubert, & Vinyard, 2005) can induce

321 indentation depths (δ) of around 7.0 and 2.8 cm based on the Hertzian contact mechanics

322 for two hemispheres (equation (13)):

323

$$\delta = (\frac{9F^2}{8R'E'^2})^{1/3} \qquad (13)$$

324

325 The extent of deformation on the tongue surface in those cases is considerable

326 compared to the tongue thickness and in this case the tongue can be considered as a soft

327 layer on top of the floor of the mouth. Relevant equations for film thickness measurement of

328 soft layered rigid materials can be obtained from a work by Dowson and Yao (1994).

329 However, the movement of the tongue and the soft nature of the sublingual salivary glands

330 and muscles of the tongue (genioglossus or hyoglossus) make the problem further complex.

331 This suggests that the developed equations for soft-layered rigid bodies might not be

332 applicable. Moreover, tongue similar to articular cartilage exhibits anisotropic, time-

333 dependent and nonlinear mechanical characteristics and the values of between 0.4-9 kPa

334 reported for its shear modules (Wang, He, Wu, & Zhang, 2018) suggests that the modulus

335 for tongue can vary depending on the loading rate and depth. Therefore, a strain-stiffening

336 property can be envisaged for tongue which mitigates large deformation under compression.

337 The "*toe stage*" that is the initial nonlinear behaviour of soft tissues has been experimentally

338 observed in tensile tests (Wang, et al., 2018).

339 Further, it is vital to perceive the methods used by state of the art tribometers to

340 generate processed data (*e.g.* friction coefficient). For example, Mini Traction Machine

341 (MTM, PCS Instruments, UK) often collects two sets of data at a specific entrainment speed,

342 where the body *a* rotates faster as compared to the body *b* during the first set and slower

343 during the second set. This method has been implemented to rule out the influence of zero

344 offset reading by the force transducer. The difference between these two sets of data has

345 been used to calculate the friction coefficient (de Vicente, et al., 2005). The Poiseuille flow

346 contribution to the viscous shear forces is independent of the sliding direction and hence

347 this method leads to the Poiseuille flow being omitted from the results. In this case, one

348 should use only the second term in the de-Vicente equation (*i.e.* $SRR(3.8U^{0.71}W^{-0.76} +$

349 $0.96U^{0.36}W^{-0.11})$) for prediction of the friction coefficient. In general, assumptions have been

350 made to derive equations and those have to be thoroughly considered for the application.

351 For example, in solving Reynolds equations often inertia and gravity forces have been

352 assumed to be negligible and slip at the boundary of the lubricant and the surfaces and non-

353 laminar flow have been regarded as unlikely/trivial which are relevant in most cases.

354

355 **Viscoelasticity of the soft body including influence on the EHL.** Prediction of the film

356 thickness and friction coefficient can become more intricate when the contribution of

357 viscoelasticity of the contact bodies plays a considerable role. The viscoelasticity of the

358 material potentially leads to asymmetric pressure distribution (Hooke & Huang, 1997) and

359 rupture/ distortion of the elasto-hydrodynamic lubricant film at the inlet of the contact (Hutt

360 & Persson, 2016). Therefore, shifting the minimum film thickness to contact inlet, whereas

361 one would usually expect the minimum film thickness to happen at the flow outlet. As shown

362 in **Figure 2** using a blue dashed line (VESM, a theoretical prediction), this eventually voids

363 the linear correlation between the friction coefficient and entrainment speed in log-log scale.

364 Upon increase in a dimensionless speed parameter *(i.e. $ut/_R$*, where t is the characteristic

365 viscoelastic relaxation time of the material) in a rigid-ball on viscoelastic disc configuration,

366 the pressure distributed in a asymmetric shape with a spike in the contact inlet propelling

367 the minimum film thickness to the lubricant inlet tend to risk a lubricant starvation (Putignano

368 & Dini, 2017). This is accompanied with the incomplete relaxation of the material at the outlet

369 region and stiffening effect of lubricant flow leading to a deviation from the Hertzian circular

contact zone and the linear correlation of friction with the logarithm of the speed (see **Figure 2**).

The study by Putignano and Dini (2017) exhibited a critical entrainment speed (u_c) for a rigid ball rolling against a soft disc configuration above which visco-elasto-hydrodynamic regime may be observed, as given by equation (14).

$$u_c = \frac{R}{\pi t}\sqrt{\frac{E_\infty}{E_0}} \qquad (14)$$

E_∞ and E_0 are glassy and rubbery elastic moduli of the material. Depending on the load and material properties (*e.g.* relatively larger t values), if it transpired that u_c falls into the hydrodynamic region, one would expect to see a classical transition of EHL to hydrodynamic regime. On the other hand, the visco-elasto-hydrodynamic regime occurs when the material deformation at u_c is comparable to the lubricant film thickness, that is $\frac{h_{Hydrostatic}}{\delta} \approx 1 \ or \ smaller$, where $h_{Hydrostatic} \propto R^3(\frac{\eta u_c}{F})^2$.

In a work by Wang, et al. (2018), the characteristic relaxation time ($t \ in \ e^{-\frac{T}{t}}$) for tongue tissue samples from boars appeared to be in the range of 80-300 s in tensile tests at a strain rate of $\sim 3 \times 10^{-5} \ s^{-1}$. The relaxation characteristic time constant observed by Wang, et al. (2018) is large and probably resulted from extremely low strain rate and relaxation modelling with a single-component exponential decay function (Abbott, Lowy, & Russell, 1957; Van Loocke, Lyons, & Simms, 2008). Unfortunately, literature lacks a comprehensive understanding of stress relaxation phenomena in human tongue. However, stress relaxation results for porcine muscle tissue have showed three characteristic relaxation time constants of sub second (10^{-5}), few seconds and order of 100 seconds (Fitzgerald, Bootsma, Berberich, & Sparks, 2015). Assuming similar relaxation time

393 constants for tongue, $\frac{E_\infty}{E_0}$ ratio of 10-100 and the tribo-contact between popcorn kernels and

394 tongue (see previous section, *i.e.* Isoviscous elastic lubrication regime), in short-lived

395 contacts (well below a second), the viscoelastic contribution seems to be unlikely as the

396 critical entrainment speed will be in the order of few hundred meters per second. However,

397 if it happened that the contact time satisfies the second stress relaxation incident (few

398 seconds), the critical speed will be in the order of few mm/s and hence deviation from

399 isoviscous elastic lubrication regime can be expected. The viscoelastic contribution can be

400 more pronounced in the tongue tip and soft palate where the greatest viscoelasticity has

401 been observed (Wang, et al., 2018). Further research works are essential to determine

402 strain-stiffening and stress relaxation behaviour (viscoelasticity/poro-viscoelasticity) of

403 tongue and to elucidate characteristic parameters of viscoelasticity (time constants). This

404 information will shed light on occasions where consideration of tongue viscoelasticity is

405 required, for example friction behaviour in the hydrodynamic lubrication regime presented

406 in **Figure 2**.

407   The above statements indicate that the hysteresis losses influence the friction

408 coefficient of the full-film regime and therefore, different friction values are expected to be

409 observed for example for a rigid-ball on soft-disc (*e.g.* popcorn kernels on tongue)

410 configuration as compared to a soft-ball on soft-disc (*e.g.* meatball on tongue) configuration.

411 This implies that elimination of hysteresis induced frictional forces should yield interfacial

412 friction forces independent of the contact configuration. This hypothesis was recently

413 implemented (Sadowski & Stupkiewicz, 2019) through estimation of frictional forces using

414 Persson's equation for rolling friction of viscoelastic materials (Persson, 2010) and

415 performing correction for the hysteresis losses. The experimental results following the

416 correction showed that the full-film interfacial friction coefficients for different configurations

417 (soft-on-hard, hard-on-soft and soft-on-soft) follow a single regression equation (equation

418 15) (Sadowski & Stupkiewicz, 2019):

419

$$\text{Friction coefficient in EHL lubrication regime, } \mu_{EHL} = 6.05(\frac{U}{W})^{0.547} \qquad (15)$$

420

421   The logarithm of the interfacial friction coefficient increased linearly with the logarithm

422   of the Hersey number ($\eta u/F$). However, as one can expect, the pressure distribution and

423   film thickness profile, where hysteresis forces play a role, alter considerably from one to the

424   other configuration and this is shown by Putignano (2020) in **Figure 2** (blue dashed line,

425   VESM). It should be noted the Persson's model (Persson, 2010) and the work by Sadowski

426   and Stupkiewicz (2019) assume negligible influence of thermal effects which impact film

427   thickness and friction (usually at high rolling/sliding speeds). This seems to be a valid

428   assumption in oral tribology considering low entrainment speeds and vascular nature of oral

429   surfaces.

430

431   **Viscoelastic effects within mixed/ boundary regimes**: The pioneering work by Bongaerts

432   et al. (2007a) showed that an empirical model can provide a 'master' curve (shown in **Figure**

433   **2**, black solid line) that embraces the influence of fluid viscosity based on the Sommerfeld

434   number (Hersey number enclosing design parameters). This approach has proved vital in

435   interpreting the fiction associated with rheologically and structurally complex food systems.

436   However, the master curve does not decipher some viscosity-dependent peculiarities in the

437   lubrication of soft viscoelastic surfaces especially in the boundary-mixed regimes (Selway,

438   Chan, & Stokes, 2017; Yakubov, McColl, Bongaerts, & Ramsden, 2009), and anticipated

439   from a theoretical model of Scaraggi and Persson (2014). For example, a work by one of

440   the co-authors showed that the boundary friction coefficients for lubricants composed of a

441   mixture of glycerol and water at different ratios were not identical (Selway, et al., 2017). This

442   was attributed to the decaying influence of viscosity on de-wetting and squeeze-out

443   dynamics of the lubricant molecules at the contact interface. This brings about a lower

444 friction coefficient in the mixed and boundary lubrication regimes as presented in **Figure 2**

445 using green dash-dotted line (VBL).

446   Further, viscoelastic deformation of roughness on soft surfaces (tongue with papillae

447 on top resembles an engineering soft material with protruding features classified as

448 roughness) results in changes in the frictional behaviour in the boundary and transition to

449 the mixed lubrication regimes. This is experimentally shown by the author where time-

450 dependant deformation of asperities on a rough viscoelastic elastomer exacerbate the

451 friction prediction in mixed lubrication regime (Selway, et al., 2017). This evidences that the

452 soft material hysteresis is of paramount importance where material deformation influences

453 lubricant flow and energy dissipation in regimes pertaining to the oral tribology (boundary to

454 EHL).

455

456 **Influence of adsorbed lubricious thin layers/moieties.** Adsorbed molecules play

457 important role in boundary friction of surfaces (see **Figure 2**, the dotted red line). In literature,

458 it has generally been suggested that greater degrees of surface coverages of self-assembly

459 monolayers bring about lower friction coefficients in macro-scale tribo tests (Fry, Moody,

460 Spikes, & Wong, 2020) which were complemented by nanoscale experiments where atomic

461 force microscopy (AFM) tips were around 20 nm (and 47 nm in post-worn condition)

462 (Brukman, Oncins, Dunbar, Boardman, & Carpick, 2006). This correlation, however, was

463 contradicted where a sharper tip of ~15 nm was used (Nalam, Pham, Castillo, & Espinosa-

464 Marzal, 2019). This is attributed to the influence of tip geometry and plowing mechanisms

465 generating defects in the adsorbed monolayer chains (Summers, Iacovella, Cummings, &

466 McCabe, 2017).

467   In the macroscale tribology, however, the influence of adsorbed thin films (*e.g.* saliva)

468 is known to impact frictional forces in boundary and mixed regimes (Krop, et al., 2019;

469 Macakova, Yakubov, Plunkett, & Stokes, 2010, 2011; Sarkar, et al., 2019a; Sarkar, et al.,

470 2017a; Yakubov, et al., 2009). Stokes, et al. (2011) showed that adsorption of

471 polysaccharides from their aqueous solution on to elastomer surfaces can reduce the

472 interfacial shear strength ($\tau_i = \frac{Friction\ force}{Contact\ area}$) between the contact bodies and therefore

473 reduce the frictional forces at the interface. This is presented in **Figure 2** where adsorbed

474 thin layers shown in red dotted line (ALTL) reduce the friction coefficient of the boundary

475 and mixed lubrication regimes. Moreover, the adsorbed thin layers may influence $u\eta_{eff}$ (*i.e.*

476 the product of entrainment speed and an effective viscosity) value where the transition

477 between mixed and hydrodynamic regimes happens (that is, $(u\eta)_{min}$). As can be seen in

478 **Figure 2** (ALTL), the transition occurred at lower values of $(u\eta)_{min}$ when there is an

479 adsorbed thin layer on the surface which was suggest to mask the effect of surface

480 roughness (Stokes, et al., 2011).

481

482 **Methodological approaches to conduct tribotests.** Overall, this section highlights the

483 importance of lubrication theories and how they can be used to understand the lubrication

484 regimes and transitions between regimes including the importance of adsorption, when

485 testing tribology of different food colloids. In tribology science, wear and frictional behaviour

486 of tribopairs which the contacts undergo are of paramount importance. In tribology of soft

487 materials, extensive attempts have been made to understand the frictional properties of

488 materials or the lubricant in between soft surfaces. This is partly due to the fact that soft

489 visco/poroelastic materials can dissipate the frictional and normal forces (through viscous

490 or (poro)elastic deformation) and hence resist against wear damages. This is also

491 accompanied with relatively lower contact pressures (primarily in the order of kPa to a few

492 MPa) that they are subjected as compared to contact pressures in tribo contacts of hard-

493 *e.g.* metallic/ceramic- materials (in the range of few tens of MPa to few GPa). The contact

494 pressure has a noticeable impact on frictional behaviour of tribo-contacts. Therefore, when

495 planning to perform tribological investigation of a material or lubricant, one needs to

familiarise themselves with the Hertzian contact mechanics and select a normal load which would yield contact pressures occurring in real conditions. Contact pressure is a function of normal load (F), contact configuration (R) and material properties ($E\ and\ v$). Contact configuration (elliptical, line or circular contacts) impacts the distribution of contact pressure along the contact area and hence, the friction. As briefly described in this section, roughness and surface topography parameters influence friction results obtained with defined contact conditions. A recently developed methodology to produce materials containing papillae-shaped features (Andablo-Reyes, et al., 2020) using soft elastomeric material has progressed the tribology of oral surface to acknowledge the influence of roughness on frictional properties of food products.

To achieve robust results, it is desirable to imitate the governing real conditions which is being investigated and implement them into the designed tribotests. Alongside contact conditions and material properties of the surfaces, it is important to consider other influencing factors. For example, an exemplary design of tribo experiments takes into account the existence or absence of pre-adsorbed saliva film in a dynamic set-up (Fan, et al., 2021). Finally cleaning procedures of materials and tribotester for tribo experiments where adsorption of moieties from lubricant onto the surfaces takes place, are crucial, as residuals of adsorbed moieties would influence frictional results.

3. Applications of oral tribology in food colloid research

From a historical perspective, oral friction has attracted attention in food colloids community due to its key role in predicting some of the textural attributes such as smoothness and creaminess (Kokini, 1987; Kokini & Cussler, 1983), which could not be understood in physical terms using rheological characterization alone. Besides achieving sensory prediction (Pradal & Stokes, 2016; Prakash, et al., 2013; Sarkar & Krop, 2019), oral tribology has gained significant momentum to address a range of unresolved challenges in food

colloid science over the last few decades. We have identified four key challenge areas *i.e.* 1) designing healthier colloids, 2) detecting food adulteration, 3) tailoring food for vulnerable population, and 4) contributing to achieving food sustainability; where oral tribology has either already acted as a catalyst to provide the underlying mechanism to some of the questions or is expected to provide new insights in the coming years. Particularly area 1 is most evolved in terms of tribological outputs as compared to 2-4 (see **Table 2** for a summary of recent studies). We summarize the recent findings in each of these challenge areas followed by raising important questions that needs to be resolved using trbological understanding.

Table 2. Summary of use of oral tribology in key food colloid applications in the last 10 years.

Hydrocolloids/ colloidal systems	Designing healthier colloids	Detecting food adulteration	Tailoring food for vulnerable population	Contributing to achieving food sustainability	References
Polysaccharides incl. dietary fibres	✓		✓		(Kieserling, Vu, Drusch, & Schalow, 2019; Kiumarsi, et al., 2019; Nguyen, Kravchuk, Bhandari, & Prakash, 2017; Stokes, et al., 2011; Torres, et al., 2019; Vieira, et al., 2020; Xu & Stokes, 2020; Zhu, Bhandari, Pang, Liu, & Prakash, 2019a; Zhu, Bhandari, & Prakash, 2018, 2019b, 2020)
Proteins	✓			✓	(Fan, Shewan, Smyth, Yakubov, & Stokes, 2021; Laiho, Williams, Poelman, Appelqvist, & Logan, 2017; Zembyla, et al., 2021; Zhu, et al., 2019b, 2020)
Emulsions	✓				(Douaire, et al., 2014; Oppermann,

et al., 2017; Upadhyay & Chen, 2019)

				References
Oil bodies	✓		✓	(Yang, et al., 2020)
Starch ghost granules	✓		✓	(Zhang, et al., 2017)
Hydrogels	✓	✓		(Hu, Andablo-Reyes, Soltanahmadi, & Sarkar, 2020; Krop, et al., 2019; Stribiţcaia, et al., 2020b)
Fluid gels	✓			(Fernández Farrés & Norton, 2015; Garrec & Norton, 2013; Hamilton & Norton, 2016)
Microgels	✓			(Andablo-Reyes, et al., 2019; Hu, et al., 2020; Sarkar, et al., 2017a; Torres, et al., 2018)
Microparticulated proteins	✓			(Liu, et al., 2016; Olivares, Shahrivar, & de Vicente, 2019)
Melamine in milk systems		✓		(Liu, Hu, Zhong, & Xu, 2018)

534

Designing healthier colloids. Due to continuous rise in obesity and overweight population around the globe and associated morbidity and mortality consequences, there has been a continual effort in food industries and research communities to replace or reduce calorie dense fat content in food. However, such reduction or replacement of fat often comes at a price of compromised textural quality, which eventually leads to rejection of the low fat and no-fat foods by consumers and thus, refutes the overall purpose of designing low calorie products. To address this, one of the strategies used by food industries has been to match the viscosity of the low fat food with the control *i.e.* high fat counterparts. Although emulating viscosity by using biopolymers, processing *etc.* have helped to match the so-called sensory thickness of the products, but it still did not have the optimized textural properties to allow matching the mouthfeel to that of the full-fat counterparts allowing the prominence of tribology in recent investigations.

547   Particularly two previous studies from separate groups (Laguna, et al., 2017a; Selway

548   & Stokes, 2013) have shown that low-fat semi-solid colloidal foods such as yoghurts,

549   custards, cream cheeses having similar viscosities to the full fat counterparts have an order-

550   of-magnitude higher boundary friction as compared to the full fat products and are perceived

551   to be less creamy. As schematically shown in **Figure 4a**, these products varying significantly

552   in fat content have similar profile of friction in the full film lubrication regimes, which is

553   expected owing to their similar viscosity profiles (Laguna, et al., 2017a; Selway & Stokes,

554   2013). However, the speed-independent frictional coefficient is significantly lower in the full

555   fat products **(Figure 4a)** due to the likely formation of a coalesced film of fat (either surface

556   shear-induced or saliva induced) (Dresselhuis, de Hoog, Cohen Stuart, Vingerhoeds, & van

557   Aken, 2008; Torres, et al., 2018) that forms a load bearing lubricating film at the interface

558   unlike the low/ no-fat products.

559
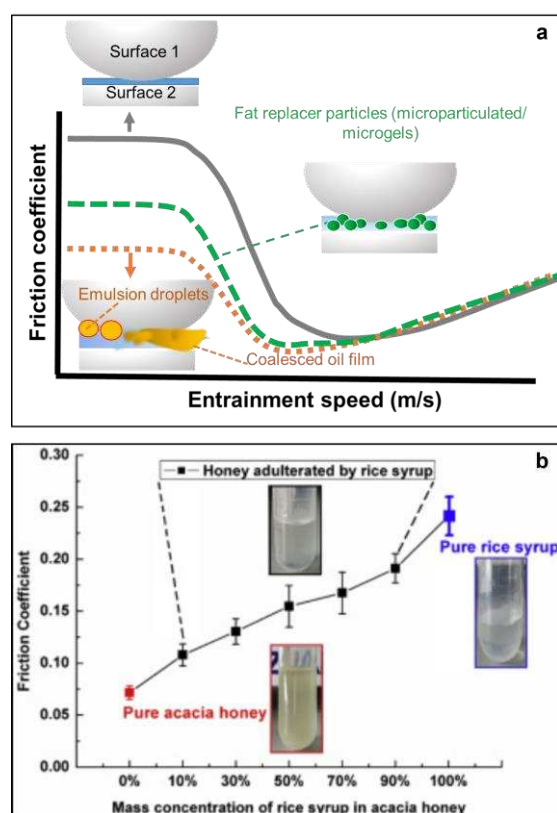
Figure 4. Examples of application of oral tribology. **a.** Schematic illustration of friction curves of fat (orange
dotted line) versus non-fat iso-viscous food products (gray solid line) (Laguna, et al., 2017a; Selway & Stokes,
2013) and replacement of fat in model foods (green dashed line) using microparticulated proteins (Liu, et al.,
2016; Olivares, et al., 2019), proteinaceous microgels (Andablo-Reyes, et al., 2019; Sarkar, et al., 2017a) or

565 biopolymeric fluid gels (Fernández Farrés & Norton, 2015; Gabriele, Spyropoulos, & Norton, 2010; Garrec &
566 Norton, 2013). **b.** Tribology used to detect rice syrup in acacia honey (Liu, Qu, Luo, Xu, & Zhong, 2019).

567
568

569   Applied research ideas to replace fat by addition of hydrocolloids (Nguyen, et al.,

570 2017), changing protein types and ratios (casein: whey protein) (Laiho, et al., 2017) in low

571 fat dairy colloids have been in the forefront of tribological research today (**Table 2**).

572 Furthermore, a key part of the formulation strategy has been to characterize the tribological

573 properties of fat mimetics to understand their ability to replace or reduce fat droplets in foods.

574 This has ranged from understanding frictional properties of diverse range of microstructures

575 of emulsion-based systems [emulsion microgel (Torres, et al., 2018), double emulsions

576 (Oppermann, et al., 2017), natural oil bodies (Yang, et al., 2020)] to polymeric microparticles

577 [microparticulated proteins (Liu, et al., 2016; Olivares, et al., 2019) (biopolymeric fluid gels

578 (Fernández Farrés & Norton, 2015; Gabriele, et al., 2010; Garrec & Norton, 2013; Hamilton

579 & Norton, 2016), microgels (Andablo-Reyes, et al., 2019; Hu, et al., 2020; Sarkar, et al.,

580 2017a; Torres, et al., 2018)] to microgel-reinforced hydrogels (Hu, et al., 2020) (**Table 2**).

581 Interestingly, many of these particles have shown interesting lubrication performance

582 (**Figure 4a**) either due to the ball-bearing mechanism of these particles emulating the

583 lubrication performance of fat-rich emulsion droplets (Liu, et al., 2016; Sarkar, et al., 2017a)

584 or due to entrainment and high shear viscosity properties of these particles (Andablo-Reyes,

585 et al., 2019; Gabriele, et al., 2010) depending upon their elasticity, size, volume fraction of

586 these particles as well as drag force of the continuum in which the particles are dispersed.

587 A recent work (Hu, et al., 2020) has shown that reinforcing hydrogels with proteinaceous

588 microgels can result in extremely high lubrication performance combining the properties of

589 high viscosity of the hydrogel and adsorption properties of the microgels, such complex

590 fluids which might find fat replacement applications in the future.

591   The other aspect of designing healthier colloids is to introduce dietary fibres in food

592 systems. Fibre addition is now pretty much a standard process in solid foods such as breads

593 and meat (Angioloni & Collar, 2011; Guedes-Oliveira, Salgado, Costa-Lima, Guedes-

594 Oliveira, & Conte-Junior, 2016), where tribology has recently been shown to be a promising

595 tool with higher friction coefficients being measured for bread containing either wheat bran

596 or resistant starch fibers as compared to control or the ones containing inulin (Kiumarsi, et

597 al., 2019) (**Table 2**). Incorporation of fibres in colloidal semi-solids is still a challenge without

598 remarkable changes in texture and sensory properties. For example, recently it was shown

599 that presence of orange peel fibre was associated with increased friction coefficients in

600 yoghurt and therefore reduced sensory smoothness depending upon size (coarse

601 ($d_{50} = 83\,\mu m$) or fine ($d_{50} = 20\,\mu m$)) and fibre concentration (0.1-1.0%) (Kieserling, et al.,

602 2019) (**Table 2**). Although one might expect this to be linked to the particulate nature of the

603 fibre particle (*e.g.* size and stiffness) increasing the roughness in the tribological contacts,

604 authors suggested the difference in tribological properties between coarse and fine fibre

605 particle-rich yoghurts to be associated with the difference in syneresis of water from the

606 continuous network. In other words, the coarse fibre-rich yoghurt released more water due

607 to a high strain associated with increased sliding speeds during tribological measurements,

608 whilst, a reduced friction coefficient in fine fibre yoghurt was attributed to spatial embedding

609 of fine fibre particles into the casein network with strong water binding properties at high

610 strain (Kieserling, et al., 2019).

611   To sum it all up, this suggests that tribology is already getting well-acknowledged in

612 research as a quintessential mechanical tool to characterize and decipher underlying

613 mechanisms of sensory perception in fat rich and reduced fat systems as well as fibre-rich

614 systems. However, many questions remain, which challenges the regular use of tribology in

615 product design. For instance, is tribology still sensitive in understanding fat replacement

616 when the degree of replacement is subtle *i.e.* difference of fat content between the low fat

617 and fat-rich systems are in the order of 5-20% that is more common in development, which

618 can be perceived orally? Also, can tribology be used to identify differences in fat-rich

products based on fatty acid profiles such as saturated fat or trans-fat versus liquid oils, in order to design healthier colloids? One might anticipate that solid fat containing mostly saturated fatty acids offering a better surface separation between oral contact surfaces similar to that of semi-solid grease. This might lead to further reduction in friction in comparison to a low viscosity liquid oil, which might slip the contact region — this needs to be investigated in the future. For fibres, the tribological studies are thus far very limited to derive broader mechanistic understanding for a wide variety of fibre-based ingredient used in formulation design.

Another important point to raise here is that often tribology has been used in monophasic model systems. However, real foods are multiphasic where a lot of formulation and processing changes are carried out to design the low-fat or high fibre systems and thus, tribology in real food systems need more focus. Lastly, a key challenge in food science is also sugar reduction. Often such replacement require use of highly sweet non-nutritive sweeteners which are required in lower quantities than sugar and also bulking agents to contribute to the total solids. Therefore a key question that remains to be answered is whether the mouthfeel issues such as metallic after taste associated with low sugar products has an underlying tribological mechanism? We believe these questions need to be resolved with more research in the domain for tribological testing to become a regularized tool in the screening process in order to accelerate product development cycle for healthier colloids.

Detecting food adulteration. Food adulteration with cheaper and sometimes even harmful ingredients and food counterfeiting is a huge economic and public health concern in many parts of the world. And, thus, easy detection of food adulteration has attracted great deal of interests among government bodies, food industries and academic institutions. Conventionally spectroscopic, chromatographic and more recently chemometric techniques are used for detection of adulteration, which are quite time consuming and generally require

30

laborious sample preparation. In last two years, tribology has been used as an impressive physical diagnostic tool to detect adulteration in food (Liu, et al., 2018; Liu, et al., 2019). For instance, Liu et al. (2019) demonstrated that that liquid acacia honey shows an elastohydrodynamic lubrication whereas rice syrup shows boundary lubrication behaviour. On adulteration of honey with rice syrup, the lubrication state changes into boundary lubrication, which can be easily quantified using any tribological set-up. As shown in **Figure 4b**, the friction coefficient of natural acacia honey becomes nearly three-time larger when rice syrup is added. Similarly, tribology was used to detect melamine in milk showing that replacement of casein by melamine can increase the friction coefficient significantly (Liu, et al., 2018) (**Table 2**), however the range of melamine investigated was 20-600 ppm. According to United Nation regulations (UN, 2012), the maximum level of melamine allowed is 1 ppm and 2.5 ppm in powdered infant formula and in other foods and animal feed, respectively. Therefore it is worth noting that the lowest concentration of melamine investigated by Liu, et al. (2018) exceeded the UN regulation already by one order of magnitude. In other words, looking at the present study (Liu, et al., 2018), tribology alone might not be able to compete in terms of detection limits with other sophisticated chromatographic techniques. Nevertheless, tribology can be a potentially cheaper and simpler screening tool for *qualitative* detection of adulterants without requiring complex sample preparation, which might need further quantification using other highly sensitive techniques. Also, for other adulterants, tribology might offer frictional distinction which needs further investigation.

These case studies provide an important as well as unique application on identifying *tribological signatures* that can be used to detect food counterfeiting or adulteration. One obvious application will be to determine adulteration with one source of milk or dairy colloids when adulterated milk from other sources, let's say buffalo milk with cow milk (Trimboli, et al., 2019). If the tribological signature *i.e.* the specific profile of the tribological curves and

671   magnitude of friction at boundary and fluid film lubrication regimes are identified for a specific

672   source of milk based on the fat content or the fatty acid profile, that would be a breakthrough

673   in milk adulteration detection as tribology can be cheaper, less time consuming and would

674   require no sample preparation as opposed to most of the techniques used in literature. To

675   realize this, it is important to carry out large scale tribological analysis on a range of fatty

676   acids as well as milks from various countries and sources in the future. The case study of

677   using tribology for adulteration detection of milk can be further translated to detection of

678   other adulterants in variety of food products.

679

680   **Tailoring food for vulnerable population.** Ageing population suffers from various forms of

681   oral insufficiencies due to physiological alteration in the oral cavity such as poor dentition,

682   lower tongue pressure, lack of saliva, which often leads to impaired oral processing and

683   eventually reduced food intake and malnutrition (Belibasakis, 2018; Laguna, Hetherington,

684   Chen, Artigas, & Sarkar, 2016; Laguna, Sarkar, & Chen, 2017b; Xu, Laguna, & Sarkar,

685   2019). Dysphagia has been a commonly diagnosed eating difficulty in swallowing or moving

686   foods and liquids from the mouth to the stomach affecting approximately 8% of the global

687   population. (Cichero, et al., 2013; Marconati, et al., 2019; Zargaraan, Rastmanesh, Fadavi,

688   Zayeri, & Mohammadifar, 2013). This has been addressed by the food community largely

689   by viscosifying liquid food by adding thickeners to increase oral residence time or increasing

690   the textural complexity of foods (Cichero, et al., 2013; Cichero, et al., 2017; Laguna, et al.,

691   2016). The key to safe swallowing of food is a complex interplay between rheological

692   properties of the bolus including bolus cohesiveness, propulsive forces applied by the

693   oropharyngeal musculature and biomechanical measures utilized for protecting the airway

694   (Foegeding, Stieger, & van de Velde, 2017; Nicosia, 2007).

695   Recently, the employment of tribology in characterization of dysphagia thickeners as

696   well as thickened food have attracted research attention (Torres, et al., 2019; Vieira, et al.,

697   2020). The fundamental work by Stokes, et al. (2011) on tribological analysis of shear

698   thinning polysaccharides such as pectin, xanthan gum, gellan gum, κ-carrageenan, and

699   locus bean gum can be considered as the basis for this challenge area (**Table 2**). It was

700   demonstrated that at the lowest sliding speeds, locust bean gum was the least lubricating

701   while pectin reduced the friction coefficient to below 0.01. It was also highlighted that

702   polysaccharides influenced the transitioning between the mixed and elastohydrodynamic

703   regimes; with pectin, gellan gum, and carrageenan showing the onset of full film lubrication

704   at significantly lower values of $u\eta_{eff}$ (entrainment speed x effective high shear rate viscosity)

705   than xanthan gum and locust bean gum. This suggests the importance of associating

706   rheology and tribology to distinguish the material performance of various thickeners.

707   In a separate study (Torres, et al., 2019), the lubrication properties of xanthan and

708   gellan gum were compared with commercial starch-based dysphagia thickeners. The

709   increase in boundary friction in presence of commercial starch-based thickeners was

710   demonstrated to be associated with α-amylase-induced hydrolysis in presence of model

711   saliva, which was not observed in gellan or xanthan gum. This study highlighted the

712   importance of gellan gum (0.3 wt%) at a much lower concentration to provide similar

713   lubrication property to that of xanthan gum (1.0 wt%). In addition to studying thickener

714   solutions on their own, the tribological performances of thickener solutions (flax seed gum,

715   xanthan gum, pregelatinized starch as well as commercial starch or xanthan-based

716   thickeners) have been investigated when incorporated in different food matrices (water, soy

717   juice and skim milk) (Vieira, et al., 2020). It was interesting to note that although the

718   lubrication performance of a particular matrix was dependent on the type and concentration

719   of the thickeners with xanthan gum showing better reduction in friction as compared to

720   starches. But more importantly, food matrices had a crucial role to play such that milk matrix

721   presented the highest lubrication performance as compared to water and soy juice

irrespective of the thickener types, highlighting the importance of studying tribology of simple thickeners as well as thickeners dispersed in real-life food matrices

These limited yet important studies show a good starting point of using tribology in addition to rheology for dysphagia management. One particular area that needs attention in the future is to study bolus tribology. The role of bolus rheology for safe swallowing is well-investigated (Chen & Lolivret, 2011; Ishihara, Nakauma, Funami, Odake, & Nishinari, 2011), but the contribution, if any, of tribology of bolus for swallowing remains to be investigated. Bolus tribology using model "*in vitro* masticated boli" *i.e.* food hydrogels + model saliva has surfaced recently (Fuhrmann, et al., 2020; Krop, et al., 2019; Stribiţcaia, et al., 2020b) but tribological analysis of real boli and correlation with swallowing time would be an obvious next step. An important milestone in this challenge area will be the incorporation of tribological parameters and/or lubrication terminologies in the International Dysphagia Diet Standardisation Initiative (IDDSI) framework (Cichero, et al., 2017), provided there is enough evidence of role of surface-induced tribology in swallowing after decoupling the rheology-dependent tribological aspects.

Contributing to achieving food sustainability. Food industries are going through a huge shift on moving towards use of plant and alternative sustainable ingredients as opposed to rather more functional animal proteins, in particular plant proteins. Besides the functional aspects, often such replacement of dairy proteins by lesser plant proteins can result in sensorial issues such as astringency which have been often underestimated (Cosson, et al., 2020). A question to raise here is that are such textural issues in plant proteins related to lubrication failure? Interestingly, a significant amount of work has been done in tribology field on astringency of polyphenol-rich wine, tea and coffee and the role of friction in quantifying astringency perception is relatively well-established. In particular, in many, if not most cases, astringency has been associated with high friction coefficients particularly in the low speed

748 regime which are either saliva-induced or surface-induced (Brossard, Cai, Osorio, Bordeu,

749 & Chen, 2016; Gibbins & Carpenter, 2013; Laguna & Sarkar, 2017; Rossetti, et al., 2009;

750 Wang, Olarte Mantilla, Smith, Stokes, & Smyth, 2020). In addition, it is well known that whey

751 protein induces astringency owing to charge interaction at low pH due to attractive

752 interactions between cationic whey protein and anionic mucins (Carter, Foegeding, & Drake,

753 2020). However, at neutral pH conditions that are relevant to dairy beverages, salivary

754 proteins pre-adsorbed to a substrate interact more with the casein than whey protein to

755 cause an increase in friction that directly related to sensory mouthfeel percepts (e.g.

756 smoothness) (Fan, et al., 2021).

757   To our knowledge there is only one study thus far from one of the co-author which

758 has looked at tribology of plant protein solutions. In this recent study (Zembyla, et al., 2021)

759 comparing soluble fractions of whey protein with pea protein showed that pea protein

760 solution does show lubrication performance at low concentrations (≤ 10 mg/mL) with high

761 and rapid rate of adsorption to the surface. However, at higher concentration, pea protein

762 solution showed aggregation transition from a polymer to a particle-like behaviour jamming

763 the contact resulting in lubrication failure. This might suggest indirectly that higher

764 concentration of pea protein might be detrimental to sensory perception resulting in

765 grittiness, dryness and astringency perception.

766   One might anticipate that tribology of plant proteins will become a key research area

767 in the future answering the governing principles behind astringency or other surface-induced

768 taste sensation of plant proteins. It is also worth noting that most plant proteins are

769 associated with polyphenols, which might also influence interaction with salivary mucins and

770 affect textural perception. One should also consider that most studies on astringency have

771 been carried out in liquids and not in solid composite foods, such as meat analogues where

772 use of plant proteins is garnering momentum. It is highly possible that such astringency

773 perception might not be pronounced when incorporated in a solid food or might be even

774 more detectable due to association with other astringent compounds. More importantly, the

775 tribological behaviour of such solid food would depend on the degree and kinetics of oral

776 processing and consequently on the length scale and time scales of the film formation

777 between the oral surfaces, which needs to be examined. Although, this area appears to be

778 at the nascent stage, we believe this will soon be populated with research due to the urgency

779 of shifting towards plant-based diets without compromising taste and textural attributes.

780

781 **4. Complementary analytical techniques for tribology**

782 Physical and chemical analytical techniques can have a profound impact in advancing our

783 fundamental understanding of food oral processing. While numerous multidisciplinary

784 approaches have been taken to address tribological phenomena across variety of

785 applications, some have provided powerful insights into the understanding of frictional

786 properties of oral-related surfaces/ substances and some have the potential to be exploited

787 in the future. In this section we aim to capture a few of these complementary tools that have

788 been used as a catalyst to explain some specific frictional behaviour in food structures or

789 allied soft materials.

790

791 **Small angle X-ray scattering (SAXS)**. Besides measuring size using dynamic light

792 scattering (DLS), small angle X-ray scattering (SAXS) can be a highly complementary tool

793 to tribology to identify the transformation of food particles during oral processing, in particular

794 to track structural changes in the range of < 100 nm length scale for colloidal dispersions

795 (Narayanan, Wacklin, Konovalov, & Lund, 2017). Although SAXS has been recently used to

796 analyse structure of food colloids and hydrocolloids (Adal, et al., 2017; Borah, Rappolt,

797 Duary, & Sarkar, 2019; Gilbert, 2019; Ramel, Peyronel, & Marangoni, 2016) and also

798 employed in combination with rheological analysis (Yu, Yakubov, Martínez-Sanz, Gilbert, &

799 Stokes, 2018) to understand conformation and intermolecular interactions in colloidal

800 systems, its use in oral tribological studies is not known to date.

801 SAXS has prompted considerable advancements in the field of soft tribology (Urueña,

802 et al., 2015). For instance, friction coefficient of polyacrylamide hydrogels (**Figure 5a**) in the

803 speed-independent regime (μ_o) has been demonstrated to inversely correlate with the mesh

804 size of the hydrogel structure (**Figure 5b**), latter obtained using SAXS (Urueña, et al., 2015).

805 On the other hand, in the speed-dependent regime, the normalized friction coefficient has

806 been found to scale with the mesh size at 1/2 power (**Figure 5c**). In machinery lubricants,

807 assessment of core diameter and aggregation of polymeric swollen nanoparticles, obtained

808 by SAXS, has led to an understanding of the boundary lubrication properties (Derry, Smith,

809 O'Hora, & Armes, 2019). This suggests that SAXS can have promising applications in

810 predicting tribological properties of food-based gels based on mesh size and degree of

811 crosslinking of the hydrocolloids as well as help understanding lubrication properties of

812 swollen food-grade microgels, which need investigation in the future.

813 Synchrotron and neutron scattering have been extensively utilised at least over the

814 last 30 years in the investigation of soft matter enabling track of (shear/ flow-induced)

815 structural changes at sub-nanometers to micron size scales (Narayanan, et al., 2017).

816 These techniques have provided a plethora of insights into the numerous areas including

817 hydrocolloids, macromolecules, where rheology and flow (Eberle and Porcar, 2012) are

818 relevant. Recently, an *in situ* shear cell with accessible scattering planes has been

819 developed to perform X-ray and neutron scattering experiments on cellulose dispersions,

820 fat crystals, caseinates in order to gain powerful insights on shear-induced changes in food

821 nanostructure (Velichko, et al., 2019). This shear cell is currently developed for "1–2 plane

822 geometry" and can be modified into cone–plate and plate–plate rheological set ups enabling

823 scattering in 1–3 plane. Nevertheless, one might anticipate that a breakthrough in this field

824 can be development of a setup that could allow probing the structural changes of bolus and

825   thin surface-adsorbed films (*e.g.* salivary films) under tribo-shear where parameters

826   including normal load (contact pressure), interactions between food and surfaces and

827   surface texture dominate the structural changes. Such hitherto unexplored approach would

828   allow gaining fundamental knowledge on real-time data on relationship between dynamics

829   of shear-induced nanostructural changes and frictional dissipation.

830

831   **Quartz crystal microbalance with dissipation monitoring (QCM-D).** Quartz crystal

832   microbalance with dissipation monitoring (QCM-D) provides information on the adsorption

833   kinetics and quantity (*via* measuring frequency shift), and viscous characteristics

834   (dissipation) of surface reactive substances in a hydrated state. The interplay between the

835   properties of adsorbed film at the interface and lubrication behaviour has been of paramount

836   importance in tribo-contacts influencing friction, wear, and corrosion performance of the

837   tribo-pairs.

838   In the last decade, QCM-D has been employed extensively in bio-relevant research

839   works (Glumac, Ritzoulis, & Chen, 2019; Hu, et al., 2020; Macakova, et al., 2010;

840   Marczynski, et al., 2020; Song, Winkeljann, & Lieleg, 2019; Xu, et al., 2020) especially in

841   skin (Farias, Hsiao, & Khan, 2020), articulating joints (Majd, et al., 2014; Morgese, Cavalli,

842   Müller, Zenobi-Wong, & Benetti, 2017; Parkes, Myant, Cann, & Wong, 2015) and food

843   science (Pradal, Yakubov, Williams, McGuckin, & Stokes, 2019; Stokes, et al., 2011; Wan,

844   et al., 2020b; Wang, et al., 2020; Zembyla, et al., 2021). In many studies, where the relevant

845   tissues are hydrophobic in nature, the microbalance sensors have been coated by PDMS

846   (Farias, et al., 2020; Pradal, et al., 2019; Song, et al., 2019; Stokes, et al., 2011; Xu, et al.,

847   2020; Zembyla, et al., 2021) usually using spin coater instruments.

848

849
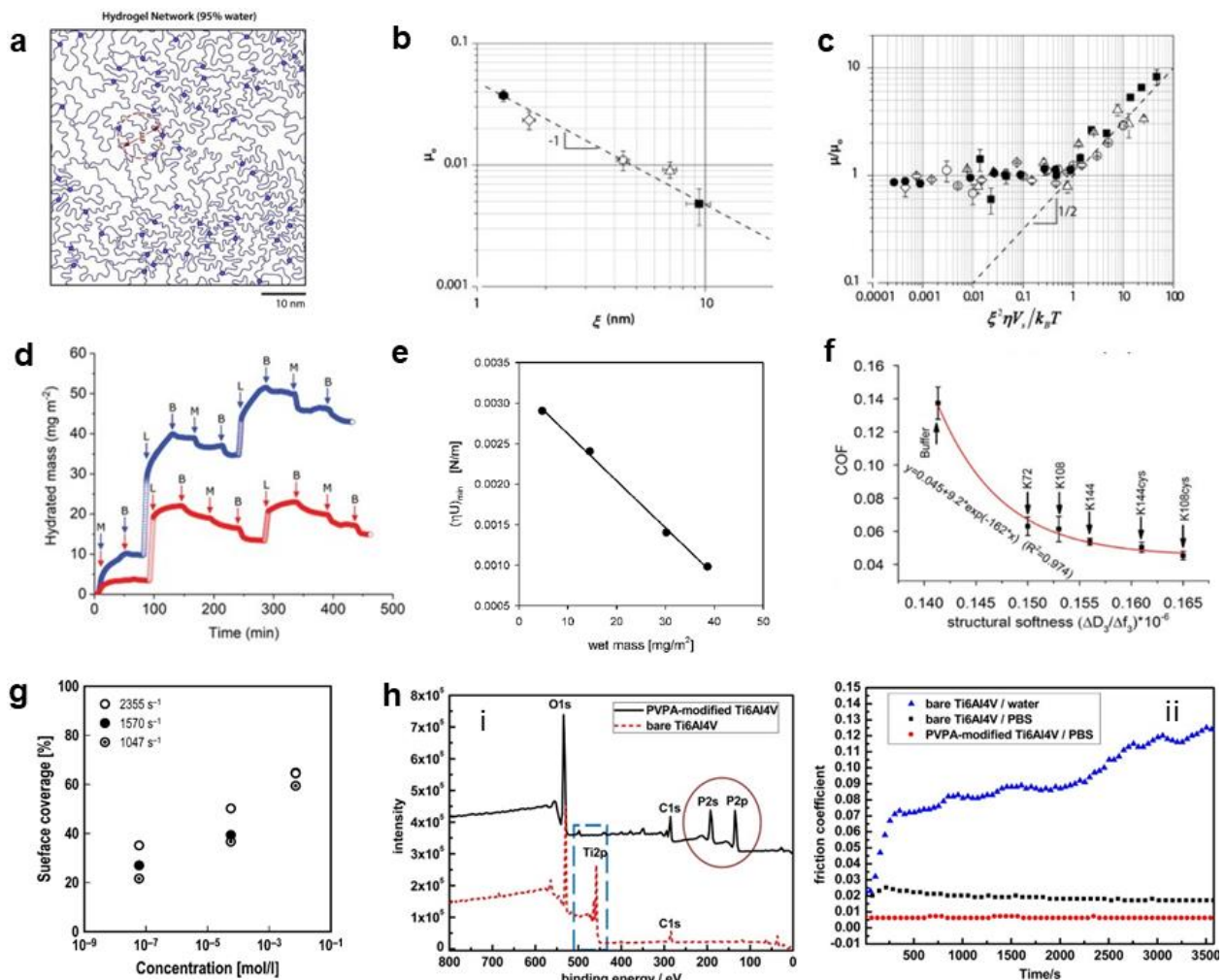
Figure 5. a) Illustration of a water-diluted polymer network (hydrogel) with a mesh size (ξ) of approximately
10 nm (Urueña, et al., 2015). b) Friction characteristics of the hydrogel in the speed-independent regime (μ_0)
was inversely correlated with mesh size data obtained by SAXS (Urueña, et al., 2015). c) The normalized
friction coefficient in the speed-dependant regime scales with the mesh size to a power of two (Urueña, et al.,
2015). d) Measurements of adsorption of salivary proteins onto hydrophobic PDMS surfaces using QCM-D at
two ionic concentrations of NaCl. The graph demonstrates incremental adsorption of hydrated mass of trilayer
of BSM/LF/BSM (Xu, et al., 2020). e) The correlation between viscosity-normalised entrainment speed at the
minimum friction coefficient in the Stribeck curve and mass (function of thickness) of the adsorbed film obtained
by QCM-D. The graph shows that adsorbed films with thicknesses in the order of the surface roughness shift
the onset of the full-film formation to lower viscosity normalised entrainment speeds (Stokes, et al., 2011). f)
The correlation between structural softness (viscoelasticity) and the friction coefficient of salivary films after
treatment with different recombinant supercharged polypeptides (SUP) and cysteine modified SUPs. A first-
order kinetic model showed that the friction coefficient exponentially decayed with the increased structural
softness as a result of SUP treatments (Wan, et al., 2020b). g) The surface coverage of adsorbed stearic acid
layers in oil lubricated tribo-contacts obtained from SPR measurements as a function of shear stress and
stearic acid concentration. The graph shows the higher concentrations of stearic acid and shear rates lead to
greater surface mass (Maegawa, Koseki, Itoigawa, & Nakamura, 2016). h) The appearance of phosphorus
signals (P 2s and P 2p) in the XPS spectrum (i) presented in black-line confirms grafting of
poly(vinylphosphonic acid) polymeric chains onto Ti6Al4V surfaces. Shown in the right panel (*i.e.* ii) using red
dotted-line, the grafting led to decreased friction coefficient (Zhang, Liu, Wen, & Wang, 2014).

870

871   For example, Xu, et al. (2020) recently designed a layered architecture of two salivary

872   proteins, that were bovine submaxillary mucin (BSM) and lactoferrin (LF), formed through

873   electrostatic interactions between the charged proteins. The binary layered system posed

874   similar lubrication and adsorption behaviour to those of human saliva (Xu, et al., 2020).

875   QCM-D data demonstrated an accumulative behaviour of adsorption, where the multiple

876   feeding of two-step injection of BSM followed by LF yielded a self-assembled bilayer, leading

877   to a stepwise increase in the hydrated mass (see **Figure 5d**). There was a relationship

878   between QCM-D data and lubrication such that the lubrication behaviour of the

879   $(BSM/LF/BSM)_n$ multilayers (where n = number of layers) at macro to nanoscale resembled

880   that of human saliva. The molecular architecture resulting in a lubricous mesh at the surface

881   quantified using QCM-D facilitated hydration and viscous lubrication mechanism with

882   possibility of energy dissipation- a structure similar to salivary pellicle comprising of an

883   anchoring sublayer and a hydrated top layer at the interface (Xu, et al., 2020).

884   QCM-D can be useful to predict the behaviour of protein films in real contacts, which

885   can offer new insights to protein tribology. Protein film formation from solutions of bovine

886   serum albumin (BSA), bovine gamma-globulin (BGG), and their mixture were studied in

887   static condition using QCM-D and in tribo-shear contacts using optical interferometry. The

888   addition of BSA to the BGG solution was shown to decay the formation of BGG films. The

889   results showed that the film thickness observed with QCM-D was different to that measured

890   by interferometry in the tribo-shear condition before and during the rolling contact. However,

891   the protein solution which engendered a greater adsorption mass and film formation rate in

892   the static condition led to thicker films in the tribo-shear condition implying Vroman effect in

893   shear conditions. The authors, therefore, postulated that the nature of the proteins in the

894   solution has a dominant influence over the protein content in the solution (Parkes, et al.,

895   2015).

896   In the area of oral tribology, lubrication properties of hydrocolloids are important,

897   which have gained interest in recent decades. The friction coefficient of aqueous solutions

898   of four polysaccharides were measured by a co-author of this paper (Stokes, et al., 2011).

A correlation between the film thickness of the hydrated polysaccharide films and viscosity-normalised entrainment speed at the minimum friction coefficient in the Stribeck curve (*i.e.* onset of the full-film formation) was observed (shown in **Figure 5e**). The adsorbed film was shown to accelerate the onset of the full-film lubrication by masking the roughness effect for relatively smooth elastomer surfaces. A more complex behaviour was observed where adsorbed film thickness assessed against lubrication properties. At the low speed range, thicker and less shear elastic films led to lower friction coefficients (Stokes, et al., 2011).

QCM-D has been used to examine the influence of the ionic strength on swelling (mass gain) and viscoelastic properties of a pectin layer covalently grafted onto PDMS surfaces through silanisation (Pradal, et al., 2019). The increase in NaCl concentration (from 1 to 100 mM) was shown to induce a thicker pectin layer and the extent of the change in thickness of the layer was shown to partially correlate with the decrease in the boundary friction depending on the degree of methyl-esterification. The shear elastic modulus of the pectin layers decreased abruptly after a certain concentration of the salt was added. This suggested that the polymer chain extension, as a result of osmotic pressure, contributes to the increase in the thickness of the layer (Pradal, et al., 2019). In this study, charge distribution of the pectin layer was postulated to be an influencing factor which limits the capability to elucidate the friction results wholly by QCM.

The findings by QCM-D do not always corroborate the findings for friction measurement instruments. This can be expected as QCM-D is a static system, which is different from the dynamic conditions and shear experienced by a sample under tribological stresses. For example, QCM-D results showed that the surface adsorption of proteoglycan-4 (lubricin) onto hydroxyapatite (HA) and collagen coated surfaces increased the friction coefficient, while lubricin adsorption on the combined surface of HA and collagen rendered a super low friction characteristics comparable to the friction coefficient observed for native cartilage (Majd, et al., 2014).

925   Other examples of complexity around exploiting QCM-D results to explain tribo

926   results can occur through interactions between different macromolecules at the interface

927   and through the influence of ionic strength which influence the surface chemistry/structure

928   of the adsorbed layer. Song, et al. (2019) found that upon addition of lysozyme to purified

929   porcine gastric mucins, the lubrication behaviour of mucin deteriorated in spite of an

930   enhanced total adsorption evidenced by QCM-D. This lack of a strong correlation was also

931   observed due to the influence of ionic strength (by addition of NaCl) on lubrication (Song, et

932   al., 2019). Further, work by Macakova, et al. (2010) showed enhanced hydration and

933   viscoelastic properties of adsorbed salivary films upon decrease of ionic strength (from a

934   physiologically relevant value obtained through a solution of 70 mM NaCl to 1-10 mM NaCl).

935   A further decrease to the minimum ionic strength (*i.e.* deionised water) led to an irreversible

936   collapse of the multi-component salivary film which illuminates the importance of interactions

937   between constituents of the salivary film. With reference to the friction results, the switch

938   from a bulk salivary solution to NaCl solutions of different ionic strengths impaired the

939   lubricity of the salivary film. This was more pronounced when the normal load was increased.

940   These observations, therefore, do not offer a conclusive correlation between viscoelastic

941   properties of film, obtained from QCM, and friction results from tribological experiments. It

942   can be inferred that more detailed and fundamental studies are vital to fully comprehend the

943   correlation (if any) between adsorption data from QCM and tribology results.

944   In recent studies (Wan, et al., 2020b; Xu, et al., 2020; Zembyla, et al., 2021), QCM

945   was used to extract the softness criteria ($\Delta D/\Delta f$) for the salivary biofilms. The increase in the

946   softness criteria translated into lower friction coefficients. A softer structure was attributed to

947   higher water contents of the biofilm and hence the hydration lubrication was accounted for

948   the enhanced lubricity. As shown in **Figure 5f**, the correlation between the softness criteria

949   and the friction coefficient was shown to follow an exponential decay function (Wan, et al.,

950   2020b).

951   Researchers should consider rheological evaluations in conjunction with QCM-D

952 when linking QCM-D with tribology results. For example, addition of thermo-responsive

953 microgels of poly(N-isopropylacrylamide)-graft-poly(ethylene glycol) (and in combination

954 with 1H-benzotriazoles) has been reported to reduce the friction coefficient of steel surfaces.

955 This was attributed to the film formation on surfaces evidenced by QCM-D (Liu, Wang, Zhou,

956 & Liu, 2013). However, the influence of apparent increases in the lubricant viscosity as a

957 result of addition of the microgel was not addressed. The lubricant viscosity directly

958 influences the film thickness (lubricant film thickness $\propto (\eta)^{0.68}$) and therefore, the impact of

959 change in viscosity, when the lubricant composition changes, should not be overlooked. In

960 other words, an increase in the lubricant viscosity can shift the lubrication conditions to less

961 harsh contact conditions resulting in a reduction in the friction coefficient.

962

963 **Surface plasmon resonance (SPR).** While gas detection and biological sensors developed

964 back in 1982 were among the first applications of the surface plasmon resonance (SPR)

965 (Chen & Ming, 2012), its current application spans from biomedical to food sciences and

966 can be used to investigate adsorption of proteins onto polymeric surfaces (Green, Davies,

967 Roberts, & Tendler, 1999). SPR utilises a laser light and detectors which track the SPR

968 angle (*i.e.* the incident angle at which the surface electrons of the substrate resonate). This

969 angle is dependent on the reflective index of the material above the substrate which

970 generates an angle shift. The angle shift is monitored in real time enabling SPR to provide

971 information on kinetics and thickness of the adsorption processes (Green, et al., 1999). Gold

972 has been commonly used as the coating for the prism due to its stability, but silver and

973 aluminium can also be used to generate the evanescent electromagnetic waves (Maegawa,

974 et al., 2016). In contrast to QCM-D, which is an acoustic based technique, the adsorption

975 data obtained from SPR represent the extent of dried mass of the adsorbate on the surface.

976 For example, the aforementioned study on the lubrication behaviour of polysaccharide

43

977 solutions (Stokes, et al., 2011) demonstrated an inverse correlation between the dry mass

978 of the polysaccharide films and their friction coefficients at the low-speed regime (*i.e.*

979 boundary to mixed) on relatively rough PDMS surfaces.

980   SPR can provide conformational information on the polymer adsorption and

981 therefore, is a useful tool to study the adsorption behaviour of salivary proteins. Navarro, et

982 al. (2020) conducted SPR using 50 and 100 nm diameter gold nanoparticles by which

983 different electromagnetic decay lengths were achieved (9 and 20 nm respectively).

984 Leveraged by detection at two different decay lengths (Navarro, Shah, & Zauscher, 2020),

985 SPR allowed for discerning a redistribution of the adsorbed polymer closer to the substrate

986 while the total mass of the layer remained constant during a phase where conformational

987 change happened.

988   The optical nature of the SPR effectuates *in situ* measurements. SPR has been used

989 against a gold sensor to monitor kinetics and evaluate the extent of tribology-induced

990 transfer films, *in situ*, from polytetrafluoroethylene, ultra-high-molecular-weight polyethylene

991 (UHMWP) and graphite solid lubricants (Krick, Hahn, & Sawyer, 2013). For instance, SPR

992 was coupled with microscopy of the wear track and confirmed the relocation of the transfer

993 film which was suggested by the decrease in the SPR reflectance (Krick, et al., 2013).

994 Another study (Maegawa, et al., 2016) investigated the adsorption kinetics of stearic acid, a

995 fatty acid used as friction modifier or corrosion inhibitor, in oil lubricated tribo-shear

996 experiments. The results showed that the static adsorption can take place over a large time

997 scale (in order of several hours). The study provided evidence that shear stresses promoted

998 the surface adsorption of stearic acid with increased shear rates leading to higher adsorption

999 mass (**Figure 5g**). The results indicated that when the surface coverage of the adsorbed

1000 layer is relatively large (> 50%), the influence of shear rate on the adsorption behaviour is

1001 sparse as compared to the influence of concentration of the fatty acid in the lubricant

1002 (Maegawa, et al., 2016) (see **Figure 5g**). These enlighten implications with reference to oral

1003 tribology, such that chewing and relative motion between tongue and palate influence

1004 parameters involved in the adsorption of saliva and macromolecules.

1005

1006 **Spectroscopic ellipsometry (SE).** Spectroscopic ellipsometry (SE) is another optical

1007 technique which estimates the film thickness based on measurement of the ratio of reflected

1008 and transmitted polarised light at an interface between materials described by Fresnel. SE

1009 is an elegant technique to measure the thickness of thin films in sub-nanometer resolution

1010 and has been widely used to decipher salivary adsorption on surfaces. Details derived by

1011 SE measurements assist in understanding tribological results. For example, SE has been

1012 used to estimate the grafting density of pectin layers grafted onto PDMS surfaces suggesting

1013 its brush-link conformation (Pradal, et al., 2019). The brush-like conformation of the grafted

1014 pectin layer was postulated to bring about lower friction coefficients as compared to

1015 adsorbed flatter pectin layers (Pradal, et al., 2019). SE can also evaluate the adsorption

1016 affinity of proteins (*i.e.* fouling) towards different surface treatments (Serrano, et al., 2013).

1017

1018 **X-ray photoelectron microscopy (XPS).** X-ray photoelectron microscopy (XPS) is a

1019 surface sensitive technique which provides information over the top 5-10 nm layer of surface

1020 films depending on the inelastic mean free path of the emitted electrons which travel through

1021 the surface. The electron trajectories are influenced by the properties of surfaces (*e.g.*

1022 atomic number) and the binding energy (BE) of signals. The chemical composition of surface

1023 films can be assessed through deconvolution of signals and contribution of each chemical

1024 bonding or element to surface films can be quantified using a sensitivity factor for each

1025 signal. A shift of binding energy in each signal imparts detailed information about the

1026 chemical composition of a specific compound.

1027   In biotribology, XPS has been used to confirm the grafting of lubricous layers. For

1028 examples, pectin bonding onto elastomer surfaces (Pradal, et al., 2019) was evidenced

through appearance of two additional peaks corresponding to acetal and carbonyl/ester-carboxylic groups. In another work, chemical bonding and stability of poly(vinylphosphonic acid) onto Ti6Al4V alloy, manifested in XPS spectra, was shown to bring about super-low friction characteristics (Zhang, et al., 2014) (see **Figure 5h**). XPS can be used to compare the grafting density and extent, for example, as a function of grafting time or concentration of monomer in a solution, or, more precisely, the ratio of the characteristic signals from the grafted substance (*e.g.* P 2p in **Figure 5h**) to the signal from the bare substrate (*e.g.* Ti 2p in **Figure 5h**) can indicate the grafting density or extent. Moreover, under certain conditions, the thickness of the grafted layer can be estimated through Ar ion or atom cluster etching. The grafting density/extent explicated by XPS can be correlated to the lubrication performance of the thin grafted layer.

Other works in this area involve pursuing XPS to assess grafting of dopamine conjugated hyaluronic acid onto polyurethane surfaces to enhance lubricity of cardiovascular catheters (Wan, Lin, Kaper, & Sharma, 2020a), grafting of 2-methacryloyloxyethyl phosphorylcholine onto the polydopamine coated surfaces to achieve anti-fouling surfaces (Asha, et al., 2019), atom transfer radical polymerization grafting of poly(N-hydroxyethylacrylamide) brushes and its crosslinking to facilitate aqueous lubrication (Zhang, et al., 2016) and grafting of cationic/anionic polyelectrolyte brushes (Han, et al., 2018). Further, adsorption processes (*e.g.* macromolecules onto surfaces of contact lenses) (Huo, Rudy, Wang, Ketelson, & Perry, 2012), and chemical reactions (*e.g.* redox reactions in preparation of silver-lignin core-shell nanoparticles) (Gan, et al., 2019) can be tracked by XPS to provide insight in to the associated lubrication performance.

Raman spectroscopy. Raman spectroscopy has been extensively used in characterisation of tribofilms from additives in oil lubricated systems (*e.g.* molybdenum dithiocarbamate) and amorphous carbon coatings. In biofilms, Raman can be used to identify the chemical

functional groups in adsorbed protein films and estimate their thickness (Zhang, Luo, Zhou, Zhang, & Huang, 2013). For example, a wear-induced change in the long-range order of the ultra-high-molecular-weight polyethylene structure was evidenced by Raman in trio-contacts relevant to motion in a prosthetic hip (Trommer, et al., 2015). In addition, oil-in-water emulsions, stabilized by a nonionic surfactant (Tween 60) was investigated by Raman spectroscopy and it was found that the volume fraction of oil was lower in the contact zone as compared to the bulk emulsion (Bongaerts, Day, Marriott, Pudney, & Williamson, 2008). Therefore, Raman spectroscopy can provide insight into tribology-induced microstructural reorientation of materials and hence can potentially be used in understanding of oral tribology processes, which to our knowledge has attracted limited attention to date.

Circular dichroism (CD). Circular dichroism (CD) spectroscopy uses circularly polarised light to provide information on optically active chiral bio-macromolecules based on the molecule's asymmetry leading to different absorption patterns depending on the direction of polarisation. Different detection techniques have been developed for CD to improve measurements spanning magnetic to liquid chromatography. Combination of CD with adsorption and lubrication data can provide detailed understanding of the lubrication behaviour of bio-macromolecules. For example, protease treatment of bovine submaxillary mucin was shown to deteriorate its low-speed lubrication properties (Madsen, Svensson, Abou Hachem, & Lee, 2015). The CD results in that work (Madsen, et al., 2015) showed almost unchanged random coil secondary structure of the treated mucin. These results suggested pivotal role of cleaved terminal un-glycosylated peptides and hydrophobic terminal domains in the lubrication behaviour of mucin.

In summary, this section encompassed a brief review of a few analytical tools that have been used in combination with tribological instrument which imparted better understanding of the frictional behaviour. However, there are numerous techniques which

have been exploited in the area of food science or tribology which are not included here; *e.g.* atomic force microscopy (AFM has been used for imaging and friction measurements (Majd, et al., 2014; Wan, et al., 2020b; Xu, et al., 2020). AFM has evidenced the disturbing influence of dietary tannins (*i.e.* epigallocatechin gallate) on friction characteristics and aggregation of whole salivary mucosal pellicle which were correlated with the tannin-induced astringency sensation (Ployon, et al., 2018). Further, some of the analytical techniques outlined above have been combined with tribometry equipment to form an integrated setup providing remarkable in situ/ real-time information under tribo-conditions such as integration with QCM (Borovsky, Garabedian, McAndrews, Wieser, & Burris, 2019), attenuated total reflection infrared (Piras, Rossi, & Spencer, 2003) and Raman (Bongaerts, et al., 2008). One might anticipate exploitation of these in-situ techniques to understand oral processes or attempts to develop new integrated setups comprising a tribo-equipment and an analysis technique valuable to investigate oral processes (*e.g.* in situ- tribo-SAXS). We envisage that this review paper, therefore, can trigger follow-up reviews or complement new method development specifically targeting complementary analytical tools used in food tribology in an integrated set-up.

5. Conclusions

Importance of oral tribology been recognized nearly four decades ago. Nevertheless, extensive research in tribology of food colloids has occurred relatively recently. This review provides a comprehensive view on lubrication theories, particularly occurring in soft contacts which are most relevant to oral surfaces that are deformable and flexible. The construction of the Stribeck curve and its variation under the changing conditions of the lubrication system (properties of the interacting surfaces and properties of the lubricant) are examined. Applications of oral (soft) tribology are still under exploration and under development, but sensory implications are no doubt core concern of most reported researches. Some

48

1107 supporting analytical techniques have also been briefly summarized in this review, in the

1108 hope that readers can make the best use of such ancillary techniques for understanding the

1109 oral tribology results.

1110   Oral tribology is still in its infancy. While new discoveries are waiting to be made, a series

1111 of serious challenges need to be addressed. Few examples of the same are given below:

1112   ● The soft surfaces in the oral environment are very unique. Despite some initial

1113   researches indicating the mechanical strength of the tongue, its dynamic firmness

1114   as a function of muscle contraction during oral processing remains largely unknown.

1115   ● Evidences show that tongue geometry and topography are highly irregular. Although

1116   there has been a significant progress in this direction on designing tongue-like

1117   papillated surface for tribometer showing the importance of random distribution of

1118   papillae on computationally studied mechanosensing (Andablo-Reyes, et al., 2020),

1119   relating the *in vitro* tribological data to real time *in vivo* sensory data remains as a

1120   challenge.

1121   ● The lubricating film in the oral environment could be highly dynamic. This is not only

1122   reflected by the changing thickness of the film, but more on the compositional level

1123   and mechanical properties of the film due to the continuous secretion of fresh saliva

1124   from different salivary glands, in flux of food, food residues and the instant food-

1125   saliva interactions.

1126   ● Huge disparities among human individuals (*e.g.* oral topography, saliva

1127   compositions, oral operational conditions, pattern of tongue movement and speed,

1128   *etc.*) are obvious and evident. Thus, reflecting such a high disparity in *in vitro*

1129   experimental design is a necessary undertaking.

1130   Of course, challenges above listed are not exclusive but just to serve examples of the

1131 challenges of oral tribology domain that need consideration in the future. We hope that this

review will lead to more discussion and experimental research on this subject and such

challenges.

Acknowledgements

CRediT author statement

Anwesha Sarkar: Conceptualization, Project administration; Data curation, Writing- Original draft preparation, Writing- Reviewing & Editing, Visualization, Supervision, Funding acquisition; **Siavash Soltanahmadi:** Conceptualization, Data curation, Writing- Original draft preparation, Writing- Reviewing & Editing, **Jianshe Chen:** Conceptualization, Writing- Reviewing & Editing; **Jason R. Stokes:** Conceptualization, Writing- Reviewing & Editing

Conflict of Interests

Declarations of interest: none

References

Abbott, B. C., Lowy, J., & Russell, F. S. (1957). Stress relaxation in muscle. *Proceedings of the Royal Society of London. Series B - Biological Sciences, 146*(923), 281-288.

Adal, E., Sadeghpour, A., Connell, S., Rappolt, M., Ibanoglu, E., & Sarkar, A. (2017). Heteroprotein complex formation of bovine lactoferrin and pea protein isolate: a multiscale structural analysis. *Biomacromolecules, 18*(2), 625-635.

Andablo-Reyes, E., Bryant, M., Neville, A., Hyde, P., Sarkar, R., Francis, M., & Sarkar, A. (2020). 3D biomimetic tongue-emulating surfaces for tribological applications. *ACS Applied Materials & Interfaces, 12*(44), 49371–49385.

Andablo-Reyes, E., Yerani, D., Fu, M., Liamas, E., Connell, S., Torres, O., & Sarkar, A. (2019). Microgels as viscosity modifiers influence lubrication performance of continuum. *Soft Matter, 15*(47), 9614-9624.

Angioloni, A., & Collar, C. (2011). Physicochemical and nutritional properties of reduced-caloric density high-fibre breads. *LWT - Food Science and Technology, 44*(3), 747-758.

Asha, A. B., Chen, Y., Zhang, H., Ghaemi, S., Ishihara, K., Liu, Y., & Narain, R. (2019). Rapid mussel-inspired surface zwitteration for enhanced antifouling and antibacterial properties. *Langmuir, 35*(5), 1621-1630.

Belibasakis, G. N. (2018). Microbiological changes of the ageing oral cavity. *Archives of Oral Biology, 96*, 230-232.

Boehm, M. W., Yakubov, G. E., Stokes, J. R., & Baier, S. K. (2020). The role of saliva in oral processing: Reconsidering the breakdown path paradigm. *Journal of Texture Studies, 51*(1), 67-77.

Bongaerts, J. H. H., Day, J. P. R., Marriott, C., Pudney, P. D. A., & Williamson, A.-M. (2008). In situ confocal Raman spectroscopy of lubricants in a soft elastohydrodynamic tribological contact. *Journal of Applied Physics, 104*(1), 014913.

Bongaerts, J. H. H., Fourtouni, K., & Stokes, J. R. (2007). Soft-tribology: Lubrication in a compliant PDMS–PDMS contact. *Tribology International, 40*(10), 1531-1542.

Borah, P. K., Rappolt, M., Duary, R. K., & Sarkar, A. (2019). Effects of folic acid esterification on the hierarchical structure of amylopectin corn starch. *Food Hydrocolloids, 86*, 162-171.

Borovsky, B. P., Garabedian, N. T., McAndrews, G. R., Wieser, R. J., & Burris, D. L. (2019). Integrated QCM-microtribometry: Friction of single-crystal MoS_2 and gold from μm/s to m/s. ACS *Applied Materials & Interfaces*, 11 (43), 40961-40969.

Brewe, D. E., & Hamrock, B. J. (1977). Simplified solution for elliptical-contact deformation between two elastic solids. *Journal of Lubrication Technology, 99*(4), 485-487.

Brossard, N., Cai, H., Osorio, F., Bordeu, E., & Chen, J. (2016). "Oral" tribological study on the astringency sensation of red wines. *Journal of Texture Studies, 47*(5), 392-402.

Brown, W. E., Eves, D., Ellison, M., & Braxton, D. (1998). Use of combined electromyography and kinesthesiology during mastication to chart the oral breakdown of foodstuffs: Relevance to measurement of food texture. *Journal of Texture Studies, 29*(2), 145-167.

Brukman, M. J., Oncins, G., Dunbar, T. D., Boardman, L. D., & Carpick, R. W. (2006). Nanotribological properties of alkanephosphonic acid self-assembled monolayers on aluminum oxide: Effects of fluorination and substrate crystallinity. *Langmuir, 22*(9), 3988-3998.

Campbell, C. L., Wagoner, T. B., & Foegeding, E. A. (2017). Designing foods for satiety: The roles of food structure and oral processing in satiation and satiety. *Food Structure, 13*, 1-12.

Carpenter, G., Bozorgi, S., Vladescu, S., Forte, A. E., Myant, C., Potineni, R. V., Reddyhoff, T., & Baier, S. K. (2019). A study of saliva lubrication using a compliant oral mimic. *Food Hydrocolloids, 92*, 10-18.

Carter, B. G., Foegeding, E. A., & Drake, M. A. (2020). Invited review: Astringency in whey protein beverages. *Journal of Dairy Science, 103*(7), 5793-5804.

Chen, J. (2009). Food oral processing—A review. *Food Hydrocolloids, 23*(1), 1-25.

Chen, J. (2014). Food oral processing: Some important underpinning principles of eating and sensory perception. *Food Structure, 1*(2), 91-105.

Chen, J., & Lolivret, L. (2011). The determining role of bolus rheology in triggering a swallowing. *Food Hydrocolloids, 25*(3), 325-332.

Chen, J., & Stokes, J. R. (2012). Rheology and tribology: Two distinctive regimes of food texture sensation. *Trends in Food Science and Technology, 25*, 4-12.

Chen, Y., & Ming, H. J. P. S. (2012). Review of surface plasmon resonance and localized surface plasmon resonance sensor. *2*(1), 37-49.

Chojnicka-Paszun, A., de Jongh, H. H. J., & de Kruif, C. G. (2012). Sensory perception and lubrication properties of milk: Influence of fat content. *International Dairy Journal, 26*(1), 15-22.

Cichero, J. A., Steele, C., Duivestein, J., Clavé, P., Chen, J., Kayashita, J., Dantas, R., Lecko, C., Speyer, R., Lam, P., & Murray, J. (2013). The need for international terminology and definitions for texture-modified foods and thickened liquids used in dysphagia management: Foundations of a global initiative. *Curr Phys Med Rehabil Rep, 1*(4), 280-291.

Cichero, J. A. Y., Lam, P., Steele, C. M., Hanson, B., Chen, J., Dantas, R. O., Duivestein, J., Kayashita, J., Lecko, C., Murray, J., Pillay, M., Riquelme, L., & Stanschus, S. (2017). Development of international terminology and definitions for texture-modified foods and

thickened fluids used in dysphagia management: The IDDSI framework. *Dysphagia, 32*(2), 293-314.

Cosson, A., Delarue, J., Mabille, A.-C., Druon, A., Descamps, N., Roturier, J.-M., Souchon, I., & Saint-Eve, A. (2020). Block protocol for conventional profiling to sensory characterize plant protein isolates. *Food Quality and Preference, 83*, 103927.

de Vicente, J., Stokes, J., & Spikes, H. (2005). The frictional properties of Newtonian fluids in rolling–sliding soft-EHL contact. *Tribology Letters, 20*(3-4), 273-286.

de Vicente, J., Stokes, J. R., & Spikes, H. A. (2006). Soft lubrication of model hydrocolloids. *Food Hydrocolloids, 20*(4), 483-491.

Derry, M. J., Smith, T., O'Hora, P. S., & Armes, S. P. (2019). Block copolymer nanoparticles prepared via polymerization-induced self-assembly provide excellent boundary lubrication performance for next-generation ultralow-viscosity automotive engine oils. *ACS Applied Materials & Interfaces, 11*(36), 33364-33369.

Devezeaux de Lavergne, M., van de Velde, F., & Stieger, M. (2017). Bolus matters: the influence of food oral breakdown on dynamic texture perception. *Food & Function, 8*(2), 464-480.

Douaire, M., Stephenson, T., & Norton, I. T. (2014). Soft tribology of oil-continuous emulsions. *Journal of Food Engineering, 139*, 24-30.

Dowson, D., & Yao, J. Q. (1994). Elastohydrodynamic lubrication of soft-layered solids at elliptical contacts: Part 2: Film thickness analysis. *Proceedings of the Institution of Mechanical Engineers, Part J: Journal of Engineering Tribology, 208*(1), 43-52.

Dresselhuis, D. M., de Hoog, E. H. A., Cohen Stuart, M. A., & van Aken, G. A. (2008). Application of oral tissue in tribological measurements in an emulsion perception context. *Food Hydrocolloids, 22*(2), 323-335.

Dresselhuis, D. M., de Hoog, E. H. A., Cohen Stuart, M. A., Vingerhoeds, M. H., & van Aken, G. A. (2008). The occurrence of in-mouth coalescence of emulsion droplets in relation to perception of fat. *Food Hydrocolloids, 22*(6), 1170-1183.

Eberle, A. P. R., & Porcar, L. (2012). Flow-SANS and Rheo-SANS applied to soft matter. *Current Opinion in Colloid & Interface Science, 17*(1), 33-43,

Fan, N., Shewan, H., Smyth, H., Yakubov, G. E., & Stokes, J. R. (2021). Dynamic Tribology Protocol (DTP): Response of salivary pellicle to dairy protein interactions validated against sensory perception. *Food Hydrocolloids*, 106478.

Farias, B. V., Hsiao, L. C., & Khan, S. A. (2020). Rheological and tribological behavior of gels and emulsions containing polymer and phospholipid. *ACS Applied Polymer Materials, 2*(4), 1623-1633.

Fernández Farrés, I., & Norton, I. T. (2015). The influence of co-solutes on tribology of agar fluid gels. *Food Hydrocolloids, 45*, 186-195.

Fitzgerald, M. M., Bootsma, K., Berberich, J. A., & Sparks, J. L. (2015). Tunable Stress Relaxation Behavior of an Alginate-Polyacrylamide Hydrogel: Comparison with Muscle Tissue. *Biomacromolecules, 16*(5), 1497-1505.

Foegeding, E. A., Daubert, C. R., Drake, M. A., Essick, G., Trulsson, M., Vinyard, C. J., & Van De Velde, F. (2011). A comprehensive approach to understanding textural properties of semi- and soft-solid foods. *Journal of Texture Studies, 42*(2), 103-129.

Foegeding, E. A., Stieger, M., & van de Velde, F. (2017). Moving from molecules, to structure, to texture perception. *Food Hydrocolloids, 68*, 31-42.

Foster, K. D., Grigor, J. M. V., Cheong, J. N., Yoo, M. J. Y., Bronlund, J. E., & Morgenstern, M. P. (2011). The role of oral processing in dynamic sensory perception. *Journal of Food Science, 76*(2), R49-R61.

Fry, B. M., Moody, G., Spikes, H. A., & Wong, J. S. S. (2020). Adsorption of organic friction modifier additives. *Langmuir, 36*(5), 1147-1155.

Fuhrmann, P. L., Aguayo-Mendoza, M., Jansen, B., Stieger, M., & Scholten, E. (2020). Characterisation of friction behaviour of intact soft solid foods and food boli. *Food Hydrocolloids*, 100, 105441.

Gabriele, A., Spyropoulos, F., & Norton, I. T. (2010). A conceptual model for fluid gel lubrication. *Soft Matter, 6*(17), 4205-4213.

Gan, D., Xing, W., Jiang, L., Fang, J., Zhao, C., Ren, F., Fang, L., Wang, K., & Lu, X. (2019). Plant-inspired adhesive and tough hydrogel based on Ag-Lignin nanoparticles-triggered dynamic redox catechol chemistry. *Nature Communications, 10*(1), 1487.

1277 Garrec, D. A., & Norton, I. T. (2013). Kappa carrageenan fluid gel material properties. Part 2:
1278   Tribology. *Food Hydrocolloids, 33*(1), 160-167.
1279 Gibbins, H. L., & Carpenter, G. H. (2013). Alternative mechanisms of astringency - What is the role
1280   of saliva? *Journal of Texture Studies, 44*, 364-375.
1281 Gilbert, E. P. (2019). Small-angle X-Ray and neutron scattering in food colloids. *Current Opinion in
1282   Colloid & Interface Science, 42*, 55-72.
1283 Glumac, M., Ritzoulis, C., & Chen, J. (2019). Surface properties of adsorbed salivary components
1284   at a solid hydrophobic surface using a quartz crystal microbalance with dissipation (QCM–
1285   D). *Food Hydrocolloids, 97*, 105195.
1286 Graca, M., Bongaerts, J. H. H., Stokes, J. R., & Granick, S. (2007). Friction and adsorption of
1287   aqueous polyoxyethylene (Tween) surfactants at hydrophobic surfaces. *Journal of Colloid
1288   and Interface Science, 315*(2), 662-670.
1289 Green, R. J., Davies, M. C., Roberts, C. J., & Tendler, S. J. B. (1999). Competitive protein
1290   adsorption as observed by surface plasmon resonance. *Biomaterials, 20*(4), 385-391.
1291 Guedes-Oliveira, J. M., Salgado, R. L., Costa-Lima, B. R. C., Guedes-Oliveira, J., & Conte-Junior,
1292   C. A. (2016). Washed cashew apple fiber (Anacardium occidentale L.) as fat replacer in
1293   chicken patties. *LWT - Food Science and Technology, 71*, 268-273.
1294 Hamilton, I. E., & Norton, I. T. (2016). Modification to the lubrication properties of xanthan gum fluid
1295   gels as a result of sunflower oil and triglyceride stabilised water in oil emulsion addition.
1296   *Food Hydrocolloids, 55*, 220-227.
1297 Hamrock, B. J. (1994). *Fundamentals of fluid film lubrication*. New York, US: McGraw-Hill, Inc.
1298 Hamrock, B. J., & Dowson, D. (1978a). Elastohydrodynamic lubrication of elliptical contacts for
1299   materials of low elastic modulus I—Fully flooded conjunction. *Journal of Lubrication
1300   Technology, 100*(2), 236-245.
1301 Hamrock, B. J., & Dowson, D. (1978b). Minimum film thickness in elliptical contacts for different
1302   regimes of fluid-film lubrication.
1303 Hamrock, B. J., & Dowson, D. (1981). Ball bearing lubrication: the elastohydrodynamics of elliptical
1304   contacts.
1305 Han, L., Yan, B., Zhang, L., Wu, M., Wang, J., Huang, J., Deng, Y., & Zeng, H. (2018). Tuning
1306   protein adsorption on charged polyelectrolyte brushes via salinity adjustment. *Colloids and
1307   Surfaces A: Physicochemical and Engineering Aspects, 539*, 37-45.
1308 Hetherington, M. M. (1996). Sensory-specific satiety and its importance in meal termination.
1309   *Neuroscience & Biobehavioral Reviews, 20*(1), 113-117.
1310 Hooke, C. J. (1995). The elastohydrodynamic lubrication of elliptical point contacts operating in the
1311   isoviscous region. *Proceedings of the Institution of Mechanical Engineers, Part J: Journal of
1312   Engineering Tribology, 209*(4), 225-234.
1313 Hooke, C. J., & Huang, P. (1997). Elastohydrodynamic lubrication of soft viscoelastic materials in
1314   line contact. *211*(3), 185-194.
1315 Hu, J., Andablo-Reyes, E., Soltanahmadi, S., & Sarkar, A. (2020). Synergistic microgel-reinforced
1316   hydrogels as high-performance lubricants. *ACS Macro Letters*, 1726-1731.
1317 Huo, Y., Rudy, A., Wang, A., Ketelson, H., & Perry, S. S. (2012). Impact of ethylene oxide butylene
1318   oxide copolymers on the composition and friction of silicone hydrogel surfaces. *Tribology
1319   Letters, 45*(3), 505-513.
1320 Hutchings, J. B., & Lillford, P. J. (1988). The perception of food texture - The philosophy of the
1321   breakdown path. *Journal of Texture Studies, 19*(2), 103-115.
1322 Hutt, W., & Persson, B. N. J. (2016). Soft matter dynamics: Accelerated fluid squeeze-out during
1323   slip. *144*(12), 124903.
1324 Ishihara, S., Nakauma, M., Funami, T., Odake, S., & Nishinari, K. (2011). Swallowing profiles of
1325   food polysaccharide gels in relation to bolus rheology. *Food Hydrocolloids, 25*(5), 1016-
1326   1024.
1327 Kieserling, K., Vu, T. M., Drusch, S., & Schalow, S. (2019). Impact of pectin-rich orange fibre on
1328   gel characteristics and sensory properties in lactic acid fermented yoghurt. *Food
1329   Hydrocolloids, 94*, 152-163.
1330 Kim, M. S., Walters, N., Martini, A., Joyner, H. S., Duizer, L. M., & Grygorczyk, A. (2020). Adapting
1331   tribology for use in sensory studies on hard food: The case of texture perception in apples.
1332   *Food Quality and Preference, 86*, 103990.

Kiumarsi, M., Shahbazi, M., Yeganehzad, S., Majchrzak, D., Lieleg, O., & Winkeljann, B. (2019). Relation between structural, mechanical and sensory properties of gluten-free bread as affected by modified dietary fibers. *Food Chemistry, 277*, 664-673.

Kokini, J. L. (1987). The physical basis of liquid food texture and texture-taste interactions. *Journal of Food Engineering, 6*(1), 51-81.

Kokini, J. l., & Cussler, E. l. (1983). Predicting the texture of liquid and melting semi-solid foods. *Journal of Food Science, 48*(4), 1221-1225.

Kokini, J. L., Kadane, J. B., & Cussler, E. L. (1977). Liquid texture perceived in the mouth. *Journal of Texture Studies, 8*(2), 195-218.

Krick, B. A., Hahn, D. W., & Sawyer, W. G. (2013). Plasmonic diagnostics for tribology: In situ observations using surface plasmon resonance in combination with surface-enhanced Raman spectroscopy. *Tribology Letters, 49*(1), 95-102.

Krop, E., Hetherington, M., Miquel-Kergoat, S., & Sarkar, A. (2018). Influence of oral processing on satiety - a systematic review and meta-analysis. *Appetite, 123*, 453.

Krop, E. M., Hetherington, M. M., Holmes, M., Miquel, S., & Sarkar, A. (2019). On relating rheology and oral tribology to sensory properties in hydrogels. *Food Hydrocolloids, 88*, 101-113.

Laguna, L., Farrell, G., Bryant, M., Morina, A., & Sarkar, A. (2017a). Relating rheology and tribology of commercial dairy colloids to sensory perception. *Food & Function, 8*, 563-573.

Laguna, L., Hetherington, M. M., Chen, J., Artigas, G., & Sarkar, A. (2016). Measuring eating capability, liking and difficulty perception of older adults: A textural consideration. *Food Quality and Preference, 53*, 47-56.

Laguna, L., & Sarkar, A. (2017). Oral tribology: update on the relevance to study astringency in wines. *Tribology - Materials, Surfaces and Interfaces, 11*, 116-123.

Laguna, L., Sarkar, A., & Chen, J. (2017b). Chapter 10 - Eating Capability Assessments in Elderly Populations. In R. R. Watson (Ed.), *Nutrition and Functional Foods for Healthy Aging* (pp. 83-98): Academic Press.

Laiho, S., Williams, R. P. W., Poelman, A., Appelqvist, I., & Logan, A. (2017). Effect of whey protein phase volume on the tribology, rheology and sensory properties of fat-free stirred yoghurts. *Food Hydrocolloids, 67*, 166-177.

Lee, S., Heuberger, M., Rousset, P., & Spencer, N. D. (2004). A tribological model for chocolate in the mouth: General implications for slurry-lubricated hard/soft sliding counterfaces. *Tribology Letters, 16*(3), 239-249.

Liu, G., Wang, X., Zhou, F., & Liu, W. (2013). Tuning the tribological property with thermal sensitive microgels for aqueous lubrication. *ACS Applied Materials & Interfaces, 5*(21), 10842-10852.

Liu, K., Stieger, M., van der Linden, E., & van de Velde, F. (2015). Fat droplet characteristics affect rheological, tribological and sensory properties of food gels. *Food Hydrocolloids, 44*, 244-259.

Liu, K., Tian, Y., Stieger, M., van der Linden, E., & van de Velde, F. (2016). Evidence for ball-bearing mechanism of microparticulated whey protein as fat replacer in liquid and semi-solid multi-component model foods. *Food Hydrocolloids, 52*, 403-414.

Liu, Y., Hu, J., Zhong, M., & Xu, W. (2018). A novel, simple and rapid method for the detection of melamine from milk based on tribology measurements. *Tribology International, 119*, 66-72.

Liu, Y., Qu, F., Luo, L., Xu, W., & Zhong, M. (2019). Detection of rice syrup from acacia honey based on lubrication properties measured by tribology technique. *Tribology International, 129*, 239-245.

Macakova, L., Yakubov, G. E., Plunkett, M. A., & Stokes, J. R. (2010). Influence of ionic strength changes on the structure of pre-adsorbed salivary films. A response of a natural multi-component layer. *Colloids and Surfaces B: Biointerfaces, 77*(1), 31-39.

Macakova, L., Yakubov, G. E., Plunkett, M. A., & Stokes, J. R. (2011). Influence of ionic strength on the tribological properties of pre-adsorbed salivary films. *Tribology International, 44*(9), 956-962.

Madsen, J. B., Svensson, B., Abou Hachem, M., & Lee, S. (2015). Proteolytic degradation of bovine submaxillary mucin (BSM) and its impact on adsorption and lubrication at a hydrophobic surface. *Langmuir, 31*(30), 8303-8309.

Maegawa, S., Koseki, A., Itoigawa, F., & Nakamura, T. (2016). In situ observation of adsorbed fatty acid films using surface plasmon resonance. *Tribology International, 97*, 228-233.

Majd, S. E., Kuijer, R., Köwitsch, A., Groth, T., Schmidt, T. A., & Sharma, P. K. (2014). Both hyaluronan and collagen type II keep proteoglycan 4 (lubricin) at the cartilage surface in a condition that provides low friction during boundary lubrication. *Langmuir, 30*(48), 14566-14572.

Malone, M. E., Appelqvist, I. A. M., & Norton, I. T. (2003). Oral behaviour of food hydrocolloids and emulsions. Part 1. Lubrication and deposition considerations. *Food Hydrocolloids, 17*(6), 763-773.

Marconati, M., Engmann, J., Burbidge, A. S., Mathieu, V., Souchon, I., & Ramaioli, M. (2019). A review of the approaches to predict the ease of swallowing and post-swallow residues. *Trends in Food Science & Technology, 86*, 281-297.

Marczynski, M., Balzer, B. N., Jiang, K., Lutz, T. M., Crouzier, T., & Lieleg, O. (2020). Charged glycan residues critically contribute to the adsorption and lubricity of mucins. *Colloids and Surfaces B: Biointerfaces, 187*, 110614.

Mo, L., Chen, J., & Wang, X. (2019). A novel experimental set up for in situ oral lubrication measurements. *Food Hydrocolloids, 95*, 396-405.

Morgese, G., Cavalli, E., Müller, M., Zenobi-Wong, M., & Benetti, E. M. (2017). Nanoassemblies of tissue-reactive, polyoxazoline graft-copolymers restore the lubrication properties of degraded cartilage. *ACS Nano, 11*(3), 2794-2804.

Mosca, A. C., & Chen, J. (2017). Food-saliva interactions: Mechanisms and implications. *Trends in Food Science & Technology, 66*, 125-134.

Myant, C., Fowell, M., Spikes, H. A., & Stokes, J. R. (2010). An investigation of lubricant film thickness in sliding compliant contacts. *Tribology Transactions, 53*(5), 684-694.

Nalam, P. C., Pham, A., Castillo, R. V., & Espinosa-Marzal, R. M. (2019). Adsorption behavior and nanotribology of amine-based friction modifiers on steel surfaces. *The Journal of Physical Chemistry C, 123*(22), 13672-13680.

Narayanan, T., Wacklin, H., Konovalov, O., & Lund, R. (2017). Recent applications of synchrotron radiation and neutrons in the study of soft matter. *Crystallography Reviews, 23*(3), 160-226.

Navarro, L. A., Shah, T. P., & Zauscher, S. (2020). Grafting to of bottlebrush polymers: Conformation and kinetics. *Langmuir, 36*(17), 4745-4756.

Nguyen, P. T. M., Kravchuk, O., Bhandari, B., & Prakash, S. (2017). Effect of different hydrocolloids on texture, rheology, tribology and sensory perception of texture and mouthfeel of low-fat pot-set yoghurt. *Food Hydrocolloids, 72*, 90-104.

Nicosia, M. A. (2007). A planar finite element model of bolus containment in the oral cavity. *Computers in Biology and Medicine, 37*(10), 1472-1478.

Nishinari, K., Fang, Y., & Rosenthal, A. (2019). Human oral processing and texture profile analysis parameters: Bridging the gap between the sensory evaluation and the instrumental measurements. *Journal of Texture Studies, 50*(5), 369-380.

Olivares, M. L., Shahrivar, K., & de Vicente, J. (2019). Soft lubrication characteristics of microparticulated whey proteins used as fat replacers in dairy systems. *Journal of Food Engineering, 245*, 157-165.

Oppermann, A. K. L., Verkaaik, L. C., Stieger, M., & Scholten, E. (2017). Influence of double (w1/o/w2) emulsion composition on lubrication properties. *Food & Function, 8*(2), 522-532.

Palczak, J., Blumenthal, D., Rogeaux, M., & Delarue, J. (2019). Sensory complexity and its influence on hedonic responses: A systematic review of applications in food and beverages. *Food Quality and Preference, 71*, 66-75.

Parkes, M., Myant, C., Cann, P. M., & Wong, J. S. S. (2015). Synovial Fluid Lubrication: The Effect of Protein Interactions on Adsorbed and Lubricating Films. *Biotribology, 1-2*, 51-60.

Pascua, Y., Koç, H., & Foegeding, E. A. (2013). Food structure: Roles of mechanical properties and oral processing in determining sensory texture of soft materials. *Current Opinion in Colloid & Interface Science, 18*(4), 324-333.

Persson, B. N. J. (2010). Rolling friction for hard cylinder and sphere on viscoelastic solid. *The European Physical Journal E, 33*(4), 327-333.

Piras, F. M., Rossi, A., & Spencer, N. D. (2003). Combined in situ (ATR FT-IR) and ex situ (XPS) study of the ZnDTP-iron surface interaction. *Tribology Letters, 15*, 181-191.

Ployon, S., Morzel, M., Belloir, C., Bonnotte, A., Bourillot, E., Briand, L., Lesniewska, E., Lherminier, J., Aybeke, E., & Canon, F. (2018). Mechanisms of astringency: Structural

1446   alteration of the oral mucosal pellicle by dietary tannins and protective effect of bPRPs.
1447   *Food Chemistry, 253*, 79-87.

1448 Pradal, C., & Stokes, J. R. (2016). Oral tribology: bridging the gap between physical
1449   measurements and sensory experience. *Current Opinion in Food Science, 9*, 34-41.

1450 Pradal, C., Yakubov, G. E., Williams, M. A. K., McGuckin, M. A., & Stokes, J. R. (2019).
1451   Responsive polysaccharide-grafted surfaces for biotribological applications. *Biotribology,*
1452   *18*, 100092.

1453 Prakash, S., Tan, D. D. Y., & Chen, J. (2013). Applications of tribology in studying food oral
1454   processing and texture perception. *Food Research International, 54*(2), 1627-1635.

1455 Prinz, J. F., & Lucas, P. W. (1997). An optimization model for mastication and swallowing in
1456   mammals. *Proceedings. Biological sciences, 264*(1389), 1715-1721.

1457 Putignano, C. (2020). Soft lubrication: A generalized numerical methodology. *Journal of the*
1458   *Mechanics and Physics of Solids, 134*, 103748.

1459 Putignano, C., & Dini, D. (2017). Soft matter lubrication: Does solid viscoelasticity matter? *ACS*
1460   *Applied Materials & Interfaces, 9*(48), 42287-42295.

1461 Ramel, P. R. R., Peyronel, F., & Marangoni, A. G. (2016). Characterization of the nanoscale
1462   structure of milk fat. *Food Chemistry, 203*, 224-230.

1463 Robinovitch, S. N., Hershler, C., Romilly, D. P. (1991). A tongue force measurement system for the
1464   assessment of oral-phase swallowing disorders. *Archives of Physical Medicine and*
1465   *Rehabilitation, 72*(1), 38-42.

1466 Rossetti, D., Bongaerts, J. H. H., Wantling, E., Stokes, J. R., & Williamson, A. M. (2009).
1467   Astringency of tea catechins: More than an oral lubrication tactile percept. *Food*
1468   *Hydrocolloids, 23*(7), 1984-1992.

1469 Rudge, R. E. D., Scholten, E., & Dijksman, J. A. (2020). Natural and induced surface roughness
1470   determine frictional regimes in hydrogel pairs. *Tribology International, 141*, 105903.

1471 Sadowski, P., & Stupkiewicz, S. (2019). Friction in lubricated soft-on-hard, hard-on-soft and soft-
1472   on-soft sliding contacts. *Tribology International, 129*, 246-256.

1473 Sarkar, A., Andablo-Reyes, E., Bryant, M., Dowson, D., & Neville, A. (2019a). Lubrication of soft
1474   oral surfaces. *Current Opinion in Colloid & Interface Science, 39*, 61-75.

1475 Sarkar, A., Kanti, F., Gulotta, A., Murray, B. S., & Zhang, S. (2017a). Aqueous lubrication, structure
1476   and rheological properties of whey protein microgel particles. *Langmuir, 33*(51), 14699-
1477   14708.

1478 Sarkar, A., & Krop, E. M. (2019). Marrying oral tribology to sensory perception: a systematic
1479   review. *Current Opinion in Food Science, 27*, 64-73.

1480 Sarkar, A., & Singh, H. (2012). Oral behaviour of food emulsions. In J. Chen & L. Engelen (Eds.),
1481   *Food Oral Processing: Fundamentals of Eating and Sensory Perception* (pp. 111-137).
1482   West Sussex, UK: Wiley-Blackwell.

1483 Sarkar, A., Xu, F., & Lee, S. (2019b). Human saliva and model saliva at bulk to adsorbed phases –
1484   similarities and differences. *Advances in Colloid and Interface Science, 273*, 102034.

1485 Sarkar, A., Ye, A., & Singh, H. (2017b). Oral processing of emulsion systems from a colloidal
1486   perspective. *Food & Function, 8*(2), 511-521.

1487 Scaraggi, M., & Persson, B. N. J. (2014). Theory of viscoelastic lubrication. *Tribology International,*
1488   *72*, 118-130.

1489 Schlich, P. (2017). Temporal Dominance of Sensations (TDS): a new deal for temporal sensory
1490   analysis. *Current Opinion in Food Science, 15*, 38-42.

1491 Selway, N., Chan, V., & Stokes, J. R. (2017). Influence of fluid viscosity and wetting on multiscale
1492   viscoelastic lubrication in soft tribological contacts. *Soft Matter, 13*(8), 1702-1715.

1493 Selway, N., & Stokes, J. R. (2013). Insights into the dynamics of oral lubrication and mouthfeel
1494   using soft tribology: Differentiating semi-fluid foods with similar rheology. *Food Research*
1495   *International, 54*, 423-431.

1496 Selway, N., & Stokes, J. R. (2014). Soft materials deformation, flow, and lubrication between
1497   compliant substrates: Impact on flow behavior, mouthfeel, stability, and flavor. *Annual*
1498   *Review of Food Science and Technology, 5*, 373-393.

1499 Serrano, Â., Sterner, O., Mieszkin, S., Zürcher, S., Tosatti, S., Callow, M. E., Callow, J. A., &
1500   Spencer, N. D. (2013). Nonfouling response of hydrophilic uncharged polymers. *Advanced*
1501   *Functional Materials, 23*(46), 5706-5718.

Sessle, B. J. (2014). Neural Basis of Oral and Facial Function. In *Reference Module in Biomedical Sciences*: Elsevier.

Shewan, H., Pradal, C., & Stokes, J. R. (2019). Tribology and its growing use toward the study of food oral processing and sensory perception. *Journal of Texture Studies, 51*(1), 7-22.

Song, J., Winkeljann, B., & Lieleg, O. (2019). The lubricity of mucin solutions is robust toward changes in physiological conditions. *ACS Applied Bio Materials, 2*(8), 3448-3457.

Sonne, A., Busch-Stockfisch, M., Weiss, J., & Hinrichs, J. (2014). Improved mapping of in-mouth creaminess of semi-solid dairy products by combining rheology, particle size, and tribology data. *LWT - Food Science and Technology, 59*(1), 342-347.

Stokes, J. R., Boehm, M. W., & Baier, S. K. (2013). Oral processing, texture and mouthfeel: From rheology to tribology and beyond. *Current Opinion in Colloid Interface Science, 18*(4), 349-359.

Stokes, J. R., Macakova, L., Chojnicka-Paszun, A., de Kruif, C. G., & de Jongh, H. H. (2011). Lubrication, adsorption, and rheology of aqueous polysaccharide solutions. *Langmuir, 27*(7), 3474-3484.

Stribeck, R. (1902). Die wesentlischen eigenschaften der gleit- und rollenlager. *Zeitschrift des Vereines deutscher Ingenieure, 46*(37 (Part I), 38 (Part II), 39 (Part III)), 1341-1348 (Part I), 1432-1438 (Part II) and 1463-1470 (Part III).

Stribiţcaia, E., Evans, C. E. L., Gibbons, C., Blundell, J., & Sarkar, A. (2020a). Food texture influences on satiety: systematic review and meta-analysis. *Scientific Reports, 10*(1), 12929.

Stribiţcaia, E., Krop, E. M., Lewin, R., Holmes, M., & Sarkar, A. (2020b). Tribology and rheology of bead-layered hydrogels: Influence of bead size on sensory perception. *Food Hydrocolloids, 104*, 105692.

Summers, A. Z., Iacovella, C. R., Cummings, P. T., & McCabe, C. (2017). Investigating Alkylsilane Monolayer Tribology at a Single-Asperity Contact with Molecular Dynamics Simulation. *Langmuir, 33*(42), 11270-11280.

Taylor, B. L., & Mills, T. B. (2020). Surface texture modifications for oral processing applications. *Biotribology, 23*, 100132.

Torres, O., Andablo-Reyes, E., Murray, B. S., & Sarkar, A. (2018). Emulsion microgel particles as high-performance bio-lubricants. *ACS Applied Materials & Interfaces, 10*(32), 26893-26905.

Torres, O., Yamada, A., Rigby, N. M., Hanawa, T., Kawano, Y., & Sarkar, A. (2019). Gellan gum: A new member in the dysphagia thickener family. *Biotribology, 17*, 8-18.

Trimboli, F., Costanzo, N., Lopreiato, V., Ceniti, C., Morittu, V. M., Spina, A., & Britti, D. (2019). Detection of buffalo milk adulteration with cow milk by capillary electrophoresis analysis. *Journal of Dairy Science, 102*(7), 5962-5970.

Trommer, R. M., Maru, M. M., Oliveira Filho, W. L., Nykanen, V. P. S., Gouvea, C. P., Archanjo, B. S., Martins Ferreira, E. H., Silva, R. F., & Achete, C. A. (2015). Multi-scale evaluation of wear in UHMWPE-metal hip implants tested in a hip joint simulator. *Biotribology, 4*, 1-11.

Tsui, S., Tandy, J., Myant, C., Masen, M., & Cann, P. M. (2016). Friction measurements with yoghurt in a simulated tongue-palate contact. *Biotribology, 8*, 1-11.

UN (2012). UN food standards body sets new regulations to help improve consumer health. United Nations News. Available from: https://news.un.org/en/story/2012/07/414772-un-food-standards-body-sets-new-regulations-help-improve-consumer-health.

Upadhyay, R., & Chen, J. (2019). Smoothness as a tactile percept: Correlating 'oral' tribology with sensory measurements. *Food Hydrocolloids, 87*, 38-47.

Urueña, J. M., Pitenis, A. A., Nixon, R. M., Schulze, K. D., Angelini, T. E., & Gregory Sawyer, W. (2015). Mesh size control of polymer fluctuation lubrication in gemini hydrogels. *Biotribology, 1-2*, 24-29.

Van Loocke, M., Lyons, C. G., & Simms, C. K. (2008). Viscoelastic properties of passive skeletal muscle in compression: Stress-relaxation behaviour and constitutive modelling. *Journal of Biomechanics, 41*(7), 1555-1566.

Velichko, E., Tian, B., Nikolaeva, T., Koning, J., van Duynhoven, J., & Bouwman, W. G. (2019). A versatile shear cell for investigation of structure of food materials under shear. *Colloids and Surfaces A: Physicochemical and Engineering Aspects, 566*, 21-28.

Vieira, J. M., Oliveira, F. D., Salvaro, D. B., Maffezzolli, G. P., de Mello, J. D. B., Vicente, A. A., & Cunha, R. L. (2020). Rheology and soft tribology of thickened dispersions aiming the

development of oropharyngeal dysphagia-oriented products. *Current Research in Food Science, 3*, 19-29.

Wan, H., Lin, C., Kaper, H. J., & Sharma, P. K. (2020a). A polyethylene glycol functionalized hyaluronic acid coating for cardiovascular catheter lubrication. *Materials & Design, 196*, 109080.

Wan, H., Ma, C., Vinke, J., Vissink, A., Herrmann, A., & Sharma, P. K. (2020b). Next generation salivary lubrication enhancer derived from recombinant supercharged polypeptides for xerostomia. *ACS Applied Materials & Interfaces, 12*(31), 34524-34535.

Wang, D., He, C., Wu, C., & Zhang, Y. (2018). Mechanical behaviors of tension and relaxation of tongue and soft palate: Experimental and analytical modeling. *Journal of Theoretical Biology, 459*, 142-153.

Wang, Q., Wang, X., & Chen, J. (2021). A new design of soft texture analyzer tribometer (STAT) for in vitro oral lubrication study. *Food Hydrocolloids, 110*, 106146.

Wang, S., Olarte Mantilla, S. M., Smith, P. A., Stokes, J. R., & Smyth, H. E. (2020). Astringency sub-qualities drying and pucker are driven by tannin and pH – Insights from sensory and tribology of a model wine system. *Food Hydrocolloids, 109*, 106109.

Williams, S. H., Wright, B. W., Truong, V. d., Daubert, C. R., & Vinyard, C. J. (2005). Mechanical properties of foods used in experimental studies of primate masticatory function. *American Journal of Primatology, 67*(3), 329-346.

Wilson, A., Luck, P., Woods, C., Foegeding, E. A., & Morgenstern, M. (2016). Comparison of jaw tracking by single video camera with 3D electromagnetic system. *Journal of Food Engineering, 190*, 22-33.

Witt, T., & Stokes, J. R. (2015). Physics of food structure breakdown and bolus formation during oral processing of hard and soft solids. *Current Opinion in Food Science, 3*, 110-117.

Xu, F., Laguna, L., & Sarkar, A. (2019). Aging-related changes in quantity and quality of saliva: Where do we stand in our understanding? *Journal of Texture Studies, 50*(1), 27-35.

Xu, F., Liamas, E., Bryant, M., Adedeji, A. F., Andablo‑Reyes, E., Castronovo, M., Ettelaie, R., Charpentier, T. V., & Sarkar, A. (2020). A self‑assembled binary protein model explains high‑performance salivary lubrication from macro to nanoscale. *Advanced Materials Interfaces, 7*(1), 1901549.

Xu, Y., & Stokes, J. R. (2020). Soft lubrication of model shear-thinning fluids. *Tribology International, 152*, 106541.

Yakubov, G. E., McColl, J., Bongaerts, J. H. H., & Ramsden, J. J. (2009). Viscous boundary lubrication of hydrophobic surfaces by mucin. *Langmuir, 25*(4), 2313-2321.

Yang, N., Feng, Y., Su, C., Wang, Q., Zhang, Y., Wei, Y., Zhao, M., Nishinari, K., & Fang, Y. (2020). Structure and tribology of κ-carrageenan gels filled with natural oil bodies. *Food Hydrocolloids, 107*, 105945.

Yu, L., Yakubov, G. E., Martínez-Sanz, M., Gilbert, E. P., & Stokes, J. R. (2018). Rheological and structural properties of complex arabinoxylans from Plantago ovata seed mucilage under non-gelled conditions. *Carbohydrate Polymers, 193*, 179-188.

Zargaraan, A., Rastmanesh, R., Fadavi, G., Zayeri, F., & Mohammadifar, M. A. (2013). Rheological aspects of dysphagia-oriented food products: A mini review. *Food Science and Human Wellness, 2*(3), 173-178.

Zembyla, M., Liamas, E., Andablo-Reyes, E., Gu, K., Krop, E. M., Kew, B., & Sarkar, A. (2021). Surface adsorption and lubrication properties of plant and dairy proteins: A comparative study. *Food Hydrocolloids, 111*, 106364.

Zhang, B., Selway, N., Shelat, K. J., Dhital, S., Stokes, J. R., & Gidley, M. J. (2017). Tribology of swollen starch granule suspensions from maize and potato. *Carbohydrate Polymers, 155*, 128-135.

Zhang, C., Liu, Y., Wen, S., & Wang, S. (2014). Poly(vinylphosphonic acid) (PVPA) on titanium alloy acting as effective cartilage-like superlubricity coatings. *ACS Applied Materials & Interfaces, 6*(20), 17571-17578.

Zhang, H. Y., Luo, J. B., Zhou, M., Zhang, Y., & Huang, Y. L. (2013). Biotribological properties at the stem–cement interface lubricated with different media. *Journal of the Mechanical Behavior of Biomedical Materials, 20*, 209-216.

Zhang, J., Xiao, S., Shen, M., Sun, L., Chen, F., Fan, P., Zhong, M., & Yang, J. (2016). Aqueous lubrication of poly(N-hydroxyethyl acrylamide) brushes: a strategy for their enhanced load bearing capacity and wear resistance. *RSC Advances, 6*(26), 21961-21968.

Zhu, Y., Bhandari, B., Pang, Z., Liu, X., & Prakash, S. (2019a). Protein concentration and hydrocolloid effect on the rheological and tribological behaviour of resulting protein solution. *LWT, 100*, 150-157.

Zhu, Y., Bhandari, B., & Prakash, S. (2018). Tribo-rheometry behaviour and gel strength of κ-carrageenan and gelatin solutions at concentrations, pH and ionic conditions used in dairy products. *Food Hydrocolloids, 84*, 292-302.

Zhu, Y., Bhandari, B., & Prakash, S. (2019b). Tribo-rheology characteristics and microstructure of a protein solution with varying casein to whey protein ratios and addition of hydrocolloids. *Food Hydrocolloids, 89*, 874-884.

Zhu, Y., Bhandari, B., & Prakash, S. (2020). Relating the tribo-rheological properties of chocolate flavoured milk to temporal aspects of texture. *International Dairy Journal, 110*, 104794.